$^{129}I/^{127}I$: A Puzzling Early Solar System Chronometer

J. Jordan, T. Kirsten, and H. Richter
Max-Planck-Institut für Kernphysik, Heidelberg, Germany

Z. Naturforsch. **35a**, 145–170 (1980); received November 12, 1979

Dedicated to Prof. H. Hintenberger on the occasion of his 70th birthday

We report I-Xe ages and other relevant xenon data for seven ordinary chondrites from H and L-groups of petrologic types 4–6, which were selected on the basis of minimum weathering and shock effects. Nevertheless, no chronological order with respect to the I-Xe ages exists among the different petrologic types. We demonstrate, however, that the degree to which the I-Xe record is preserved in these chondrites, but not necessarily the age, is dependent on the thermal metamorphic history. In order to explain the lack of chronological order among the chondrites, spatiotemporal variations in the condensation-accretion process or inhomogeneities in the isotopic composition of iodine in the solar nebula is required.

Introduction

The presence of excess ^{129}Xe in meteorites now known to result from the decay of extinct (17 m.y. half-life) r-process produced ^{129}I, places important constraints on nucleosynthesis models and their relationship to early solar system chronology. The correlation of the excess ^{129}Xe with I-sites in meteoritic minerals was first demonstrated by Jeffery and Reynolds [1]. Afterwards, Podosek [2] showed that for some fifteen meteorites the initial $(^{129}I/^{127}I)_0$ ratio at the time of Xe-retention was variable and could be used to calculate "formation" age differences. This was accomplished by comparing the slopes of high temperature correlation lines to that for the standard, Bjurböle (L 4), for which the $(^{129}I/^{127}I)_0$ ratio was determined. The width of this interval was found to be ~ 15 m.y. indicating that meteorite formation was completed within this length of time. Formation time in this sense refers actually to the time at which xenon began to be retained in the I-bearing mineral phases, so that most of this time interval is thought to be taken up by metamorphism whereas the time for accretion itself is considered to be comparatively short [3]. Employing the meteorite classification scheme of Van Schmus and Wood [4] where increasing degree of metamorphism is characterized by assigning numbers from 1–6, Podosek [2] observed that there was no petrologic sequence of increasing metamorphic grade towards younger ages as would be expected if indeed metamorphism were responsible for most of the interval. Nevertheless, the "oldest" object was the only slightly metamorphosed carbonaceous chondrite Karoonda (C 4). Herzog et al. [5], and Lewis and Anders [6] separated magnetites from the even more primitive carbonaceous chondrites Orgueil (C 1) and Murchison (C 2) which were probably never metamorphosed, and found by I-Xe dating that they were indeed older than Karoonda by some 2–3 m.y. Since the magnetites were believed to be direct condensates from the solar nebula, the initial $(^{129}I/^{127}I)_0$ ratio was interpreted to be that at the onset of condensation. More recently, however, Drozd and Podosek [7] found an I-Xe age for an ordinary chondrite, Arapahoe (L 5), which was some 3 m.y. older than the Orgueil and Murchison magnetites, challenging the above interpretation. Our work has been primarily inspired by the lack of correlation between petrologic type and I-Xe age. A large number of the meteorites for which I-Xe data exist are shocked (Arapahoe was shocked [8]) and weathered. The role of these effects in the xenon systematics is unknown and was ignored at the time when establishing whether or not the I-Xe correlation in many meteorites existed at all was most important. We have followed the suggestion of Pellas [9] that perhaps through a careful meteorite selection avoiding these effects, the correlation between metamorphic grade and I-Xe ages could be established. Based on preliminary data evaluation, we have previously reported that even after such careful selection the correlation still fails to exist [10, 11].

Reprint requests to Dr. J. Jordan, Postfach 10 39 80, D-6900 Heidelberg 19.

0340-4811 / 80 / 0200-0145 $ 01.00/0. — Please order a reprint rather than making your own copy.

In this paper we give the final and complete data and summarize the results for those cases in which a high temperature correlation was found. Uncorrelated cases shall be reported separately. As a companion goal, we are seeking to assemble a more complete set of chronometers for the same meteorites. Pu-Xe has been measured and (Pu/U) ratios determined for four of the seven meteorites reported here [12]. ^{40}Ar-^{39}Ar analyses have been made for minerals from the same aliquot as used in the I-Xe and Pu-Xe analyses [13].

Experimental

a) General Procedures

The meteorites of this study were irradiated in two separate irradiations in the FR 2 reactor in Karlsruhe: Nadiabondi and Menow were irradiated with a nominal thermal neutron fluence of 3.9×10^{19} cm^{-2} which shall be hereafter referred to as the K-1 irradiation, and Beaver Creek, Ambapur Nagla Kernouve, Ausson, and Peetz were irradiated together with a nominal neutron fluence of 1.3×10^{19} cm^{-2} hereafter referred to as the K-2 irradiation. Coarsely broken fragments of each meteorite were wrapped in Al-foil and sealed in a quartz capsule along with Bjurböle, the age standard for these irradiations. The Bjurböle aliquot was composed of sand size grains, the < 15 μm fraction of which was removed by sieving to minimize recoil effects. Flux monotoring was accomplished by measuring the activity of ^{59}Fe produced in the reaction $^{58}Fe(n, \gamma)^{59}Fe$ in Fe-wires sealed in the capsules along with the meteorite and Bjurböle standard *. The fluxes relative to Bjurböle are shown in Table 1 and were included in the age calculations. They indicate only minor flux gradients along the length of the ampoule. Gases were extracted in a molybdenum crucible heated by RF induction in a series of 40-minute 100 °C temperature steps beginning at 600 °C (some 50 °C steps were made at higher temperatures for the K-2 samples) and ending at 1500 °C, followed by two 20 minute extractions at 1600 °C and 1650 °C. The last (1650 °C) step served to ensure that the samples were completely degassed. Reactive gases were gettered by exposure to hot Ti-getters. All of the xenon and some of the krypton were absorbed at liquid N_2 temperature on a glass U-tube. The remaining gases (He, Ne, Ar, and the remainder of the Kr) were not pumped away, but their partial pressures were substantially reduced because the volume to which the xenon was removed was small compared to the rest of the extraction and cleaning system. The mass spectrometer (described by Haag [14]) with a sensitivity and mass resolution especially suitable for xenon measurements was a metal-glass instrument with a 20 cm deflection radius operated in the static mode. Instrumental sensitivity ($\sim 2 \times 10^{-14}$ cm^3/mV) and mass discrimination ($\sim 1\%$/mass unit) were determined by analysis of air Xe pipettes.

* Although a number of stable Fe isotopes feed the ^{59}Fe activity via chain reactions during the neutron irradiation, it can be shown that for the flux used, the main production of ^{59}Fe is due to the original abundance of ^{58}Fe in the Fe-wire, other contributions being negligible.

Table 1. Thermal neutron flux relative to that received by the respective Bjurböle standard.

Irradiation	Meteorite	$(\Phi_{Met}/\Phi_{Bju})^a$
K-1	Menow	1.02
	Nadiabondi	0.99
K-2	Beaver Creek	0.94
	Ambapur Nagla	0.99
	Kernouve	1.03
	Ausson	0.98
	Peetz	0.99

[a] Determined from ^{59}Fe activity in Fe-wires. — Errors in ratios are 3%.

b) The Bjurböle Standard

It is assumed throughout this work that Bjurböle had an initial iodine ratio of $(^{129}I/^{127}I)_0 = 1.09 \times 10^{-4}$ [2]. Since one Bjurböle standard accompanied each one of the seven meteorites of this work, we can provide the largest single assembly of multiple independent I-Xe data for one single meteorite heretofore published which enables us to acquire a well founded picture concerning the reproducibility of the whole I-Xe method.

An independent test of the stability of the $(^{129}I/^{127}I)_0$ ratio within an aliquot is to compare the slopes of the high temperature correlations $(^{129}Xe^*/^{128}Xe^*)$ produced under different neutron flux conditions, where $^{129}Xe^*$ is from ^{129}I and $^{128}Xe^*$ is produced in the reactor from $^{127}I(n, \gamma\beta^-)^{128}Xe^*$. The ratio $M \equiv (^{129}Xe^*/^{128}Xe^*)$ is inversely proportional to the fluence F; therefore, for a "perfect" standard for which M is *only* dependent on the

Table 2. $(^{129}Xe^*/^{128}Xe^*)_n/(^{129}Xe^*/^{128}Xe^*)_1$ and F_1/F_n for irradiated Bjurböle standard [a].

n [b]	$(^{129}Xe^*/^{128}Xe^*)_n/(^{129}Xe^*/^{128}Xe^*)_1$	F_1/F_n [c]	^{59}Fe-Activity (10^4 CPM/mg Fe)
	K-2		
1 (Peetz)	≡ 1	≡ 1	3.844
2 (Ausson)	0.974 ± 0.063	0.960	4.004
3 (Kernouve)	0.924 ± 0.059	0.942	4.081
4 (Ambapur Nagla)	0.894 ± 0.054	0.888	4.329
5 (Beaver Creek)	0.857 ± 0.053	0.884	4.348
	K-1		
6 (Menow)	0.305 ± 0.019	0.311	(12.360) [d]
7 (Nadiabondi)	0.285 ± 0.033	0.290	(13.255) [d]

[a] $(^{129}Xe^*/^{128}Xe^*)$ is the slope of the high temperature correlation line (see text). F is the neutron fluence determined from ^{59}Fe activity in Fe-wires.

[b] The number n is an arbitrary label for individual capsules. In parentheses is the name of the meteorite in the same capsule so that reference to the $^{129}Xe^*/^{128}Xe^*$ ratio may be made from Figures 4–10.

[c] Errors in ratios are 3%.

[d] Adjusted for activity build up difference due to irradiation time differences (7d vs. 2d).

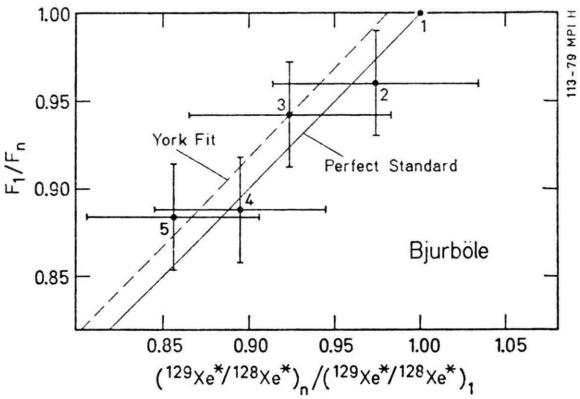

Fig. 1. Correlation of the $(^{129}Xe^*/^{128}Xe^*)$ ratio, as measured in the correlated high temperature fractions of various Bjurböle standards from the K-2 irradiation, with the inverse of the applied neutron fluence F. The data are presented relative to the sample 1 which received the lowest fluence of all n samples. The solid line gives the expected position for a perfect standard to which the fitted line comes very close. The actual fit of the data includes two standards from the K-1 irradiation with approximately 3 times higher fluences (see Table 1), but it is evident that even for the small fluence variations among K-2 samples the data follow the perfect standard line.

fluence, a plot of M_n/M_1 versus F_1/F_n should give a positive correlation with a slope of 1 and an intercept of zero (Index 1 refers to a reference irradiation). Variations in the ratio $(^{129}Xe^*/^{128}Xe^*)$ observed for the Bjurböle standard within the single irradiation K-2 and, of course, between K-1 and K-2 were, as expected, positively correlated with the inverse of the fluence (determined independently from the ^{59}Fe activity). In Table 2 the data are presented, normalized to the Bjurböle standard for Peetz, which had the highest $(^{129}Xe^*/^{128}Xe^*)$ ratio and the lowest fluence. A fit of the data yields a slope of 1.02 ± 0.02 and an intercept of 0.00 ± 0.01 shown as a dotted line in Fig. 1, in very good agreement with what one expects from a perfect standard (solid line).

With only two exceptions all Bjurböle $^{132}Xe_t$ (t ≡ trapped) contents lie within 5 percent of one another with an average of 5.4×10^{-10} cm^3 STP/g, and the average $^{129}Xe/^{132}Xe$ ratio after fission and spallation corrections (see *Results and Data System Reduction*) for all Bjurböle standards is 1.755 ± 0.008. The average trapped $(^{129}Xe/^{132}Xe)_t$ ratio determined from the I-Xe correlation diagram and an assumed $(^{128}Xe/^{132}Xe)_t = 0.082$ (Murray composition [15]) is 1.062 ± 0.008. Iodine and tellurium contents determined from the neutron activation (see *I and Te Contents*) tend to cluster reasonably well (within 20 percent) around their average values. These data are summarized in Table 19. The two exceptional Bjurböle standards (for Beaver Creek and Ausson) contain about 20 percent more $^{132}Xe_t$ than the average. Their total $(^{129}Xe/^{132}Xe)$ ratios, however, (1.742 and 1.768) are near the Bjurböle average. The Bjurböle for Ausson is also enhanced in the I and Te contents.

Results and Data System Reduction

The results are summarized in Tables 3a, b to Tables 9a, b. Since the I-Xe correlation diagram depends on the two component model assumption of trapped gas plus I-correlated gas, the measured $(^{128}Xe/^{132}Xe)$ and $(^{129}Xe/^{132}Xe)$ ratios are traditionally corrected for the presence of other components. Our approach follows basically that outlined by Podosek [2], but some simplifications were employed where they were warranted by the data. We clarify these corrections as follows:

a) Blank Corrections

Blanks were run at 1500 °C for 40 minutes before and after each sample and Bjurböle standard and

Table 3a. Xenon in irradiated Menow (H 4) 2.075 g.

Temp. (°C)	[132] $\times 10^{-12}$ (cm^3 STP/g)	$^{124}Xe/^{132}Xe$	$^{126}Xe/^{132}Xe$	$^{128}Xe/^{132}Xe$	$^{129}Xe/^{132}Xe$	$^{130}Xe/^{132}Xe$	$^{131}Xe/^{132}Xe$	$^{134}Xe/^{132}Xe$	$^{136}Xe/^{132}Xe$
Blank	0.06 ± 0.01			0.788 ± 0.249	1.123 ± 0.174	0.148 ± 0.017		0.219 ± 0.042	0.428 ± 0.107
600	9.0	0.0033 ± 0.0001	0.0032 ± 0.0005	8.44 ± 0.06	0.872 ± 0.005	0.130 ± 0.002	3.72 ± 0.03	0.639 ± 0.007	0.736 ± 0.006
700	2.1	0.0017 ± 0.0007		2.35 ± 0.03	0.296 ± 0.009	0.0452 ± 0.0031	6.31 ± 0.06	1.388 ± 0.013	1.983 ± 0.016
800	1.9	0.0004 ± 0.0005	0.0076 ± 0.0012	3.26 ± 0.05	0.627 ± 0.018	0.0835 ± 0.0054	7.53 ± 0.10	0.857 ± 0.012	1.238 ± 0.031
900	4.4	0.0016 ± 0.0004	0.0045 ± 0.0003	2.08 ± 0.05	0.875 ± 0.026	0.0983 ± 0.0039	5.40 ± 0.17	1.197 ± 0.032	1.345 ± 0.038
800(2)	100.5	0.00341 ± 0.00003	0.00350 ± 0.00003	0.06103 ± 0.00007	0.9585 ± 0.0017	0.1518 ± 0.0006	0.795 ± 0.002	0.3869 ± 0.0009	0.3326 ± 0.0009
900(2)	32.9	0.0037 ± 0.0001	0.0037 ± 0.0001	0.0773 ± 0.0007	0.948 ± 0.003	0.152 ± 0.001	0.809 ± 0.004	0.377 ± 0.003	0.327 ± 0.003
1000	47.6	0.0044 ± 0.0001	0.0046 ± 0.0001	0.0934 ± 0.0008	0.967 ± 0.004	0.151 ± 0.001	0.849 ± 0.003	0.389 ± 0.002	0.339 ± 0.002
1100	123.6	0.0036 ± 0.0001	0.00322 ± 0.00006	0.1202 ± 0.0006	0.972 ± 0.003	0.1491 ± 0.0008	0.896 ± 0.003	0.403 ± 0.001	0.363 ± 0.001
1100(2)	28.4	0.0036 ± 0.0001	0.0033 ± 0.0001	0.194 ± 0.002	0.981 ± 0.005	0.1502 ± 0.0002	0.965 ± 0.006	0.406 ± 0.004	0.376 ± 0.003
1200	59.1	0.0029 ± 0.0003	0.0030 ± 0.0014	0.291 ± 0.002	1.039 ± 0.003	0.1448 ± 0.0003	1.138 ± 0.002	0.419 ± 0.002	0.4076 ± 0.0008
1300	46.7	0.0040 ± 0.0002	0.0040 ± 0.0007	0.700 ± 0.003	1.230 ± 0.005	0.151 ± 0.001	1.585 ± 0.006	0.464 ± 0.002	0.473 ± 0.002
1400	53.2	0.0047 ± 0.0002	0.0052 ± 0.0003	0.845 ± 0.003	1.331 ± 0.005	0.153 ± 0.002	1.584 ± 0.004	0.446 ± 0.003	0.433 ± 0.003
1500	98.2	0.00440 ± 0.00007	0.0041 ± 0.0003	0.885 ± 0.002	1.331 ± 0.003	0.1580 ± 0.0005	1.266 ± 0.004	0.424 ± 0.001	0.410 ± 0.002
1600	13.2	0.0042 ± 0.0003	0.0041 ± 0.0003	0.907 ± 0.008	1.355 ± 0.012	0.1575 ± 0.0024	1.174 ± 0.009	0.442 ± 0.025	0.475 ± 0.007
1650	4.2	0.0036 ± 0.0008	0.0033 ± 0.0008	0.997 ± 0.012	1.452 ± 0.014	0.150 ± 0.004	1.13 ± 0.02	0.436 ± 0.006	0.416 ± 0.006
	625.0								

Table 3b. Xenon in irradiated Bjurböle for Menow 1.187 g.

Temp. (°C)	[132] $\times 10^{-12}$ (cm^3 STP/g)	$^{124}Xe/^{132}Xe$	$^{126}Xe/^{132}Xe$	$^{128}Xe/^{132}Xe$	$^{129}Xe/^{132}Xe$	$^{130}Xe/^{132}Xe$	$^{131}Xe/^{132}Xe$	$^{134}Xe/^{132}Xe$	$^{136}Xe/^{132}Xe$
Blank	0.11 ± 0.03			0.788 ± 0.249	1.123 ± 0.174	0.148 ± 0.017		0.219 ± 0.042	0.428 ± 0.107
600	7.9	0.0029 ± 0.0005	0.0021 ± 0.0003	11.8 ± 0.3	1.054 ± 0.033	0.127 ± 0.004	5.10 ± 0.14	0.456 ± 0.011	0.415 ± 0.010
700	4.3	0.0862 ± 0.0173	0.1354 ± 0.0297	3.046 ± 0.011	1.369 ± 0.012	0.200 ± 0.008	4.431 ± 0.025	0.538 ± 0.010	0.508 ± 0.009
800	8.2	0.0007 ± 0.0003	0.0004 ± 0.0003	2.95 ± 0.02	0.3514 ± 0.0035	0.0439 ± 0.0019	4.548 ± 0.004	1.165 ± 0.013	1.897 ± 0.017

able 3b (continued).

emp. C)	[132] $\times 10^{-12}$ (cm³ STP/g)	$^{124}Xe/^{132}Xe$	$^{126}Xe/^{132}Xe$	$^{128}Xe/^{132}Xe$	$^{129}Xe/^{132}Xe$	$^{130}Xe/^{132}Xe$	$^{131}Xe/^{132}Xe$	$^{134}Xe/^{132}Xe$	$^{136}Xe/^{132}Xe$
00	3.5	0.0031 ± 0.0007	0.0012 ± 0.0010	9.41 ± 0.10	1.138 ± 0.016	0.108 ± 0.003	8.40 ± 0.11	0.898 ± 0.007	1.185 ± 0.009
00	7.9	0.0037 ± 0.0006	0.0035 ± 0.0006	5.20 ± 0.04	1.273 ± 0.017	0.134 ± 0.003	5.487 ± 0.032	0.700 ± 0.007	0.846 ± 0.009
00	16.7	0.0043 ± 0.0005	0.0036 ± 0.0005	3.17 ± 0.01	1.695 ± 0.015	0.147 ± 0.002	2.870 ± 0.024	0.528 ± 0.007	0.524 ± 0.004
00	94.9	0.0041 ± 0.0001	0.00385 ± 0.00009	2.262 ± 0.004	1.820 ± 0.006	0.1586 ± 0.0009	1.628 ± 0.004	0.408 ± 0.002	0.3725 ± 0.0015
00	132.1	0.0046 ± 0.0001	0.0041 ± 0.0001	2.597 ± 0.005	1.943 ± 0.004	0.1699 ± 0.0009	1.257 ± 0.004	0.412 ± 0.002	0.374 ± 0.002
00	134.7	0.0046 ± 0,0002	0.0043 ± 0.0001	1.124 ± 0.002	1.405 ± 0.004	0.162 ± 0.001	0.962 ± 0.002	0.387 ± 0.001	0.348 ± 0.002
00	111.7	0.0036 ± 0.0001	0.0034 ± 0,0002	1.571 ± 0.006	1.575 ± 0.006	0.163 ± 0.001	0.918 ± 0.005	0.405 ± 0.002	0.379 ± 0.002
00	7.3	0.0017 ± 0.0007	0.0012 ± 0.0009	1.97 ± 0.02	1.595 ± 0.022	0.162 ± 0.004	1.026 ± 0.011	0.4395 ± 0.0065	0.412 ± 0.006
50	4.6	0.0045 ± 0.0009	0.0041 ± 0.0009	2.17 ± 0.08	1.807 ± 0.016	0.149 ± 0.006	1.086 ± 0.006	0.408 ± 0.008	0.418 ± 0.008
	533.8								

able 4a. Xenon in irradiated Nadiabondi (H 5) 2.081 g.

emp. C)	[132] $\times 10^{-12}$ (cm³ STP/g)	$^{124}Xe/^{132}Xe$	$^{126}Xe/^{132}Xe$	$^{128}Xe/^{132}Xe$	$^{129}Xe/^{132}Xe$	$^{130}Xe/^{132}Xe$	$^{131}Xe/^{132}Xe$	$^{134}Xe/^{132}Xe$	$^{136}Xe/^{132}Xe$
lank	0.024 ± 0.014	0.0082 ± 0.0328	0.0042 ± 0.0049	0.265 ± 1.706	0.728 ± 0.400	0.273 ± 0.159	0.391 ± 0.464		
00	5.3	0.0011 ± 0.0002	0.0012 ± 0.0003	7.91 ± 0.08	1.077 ± 0.008	0.168 ± 0.002	4.675 ± 0.044	0.429 ± 0.005	0.396 ± 0.004
00	3.0	0.0005 ± 0.0004	0.0006 ± 0.0003	1.69 ± 0.02	0.153 ± 0.005	0.0309 ± 0.0022	3.227 ± 0.035	1.584 ± 0.018	2.403 ± 0.023
00	1.4			4.42 ± 0.08	0.230 ± 0.006	0.0507 ± 0.0032	6.618 ± 0.076	1.580 ± 0.022	2.184 ± 0.080
00	2.3	0.0006 ± 0.0002	0.0006 ± 0.0002	4.96 ± 0.16	0.675 ± 0.025	0.1045 ± 0.0053	8.54 ± 0.32	1.060 ± 0.032	1.388 ± 0.041
00	7.9	0.0065 ± 0.0007	0.0041 ± 0.0008	2.10 ± 0.02	1.229 ± 0.006	0.149 ± 0.003	5.20 ± 0.04	0.515 ± 0.009	0.502 ± 0.008
00	22.5	0.0049 ± 0.0003	0.0055 ± 0.0004	1.112 ± 0.006	1.318 ± 0.006	0.1607 ± 0.0008	2.678 ± 0.015	0.380 ± 0.003	0.342 ± 0.005
00	71.2	0.00447 ± 0.00004	0.0046 ± 0.0002	0.596 ± 0.002	1.223 ± 0.003	0.168 ± 0.001	1.531 ± 0.004	0.385 ± 0.002	0.3373 ± 0.0005
00	79.8	0.00478 ± 0.00009	0.0048 ± 0.0003	0.565 ± 0.002	1.224 ± 0.002	0.1678 ± 0.0008	1.322 ± 0.004	0.387 ± 0.001	0.3397 ± 0.0009
00	74.9	0.0045 ± 0.0001	0.0047 ± 0.0007	0.495 ± 0.001	1.183 ± 0.003	0.165 ± 0.001	1.1763 ± 0.0007	0.3885 ± 0.0010	0.345 ± 0.001
00	70.9	0.0044 ± 0.0002	0.0034 ± 0.0006	0.429 ± 0.001	1.135 ± 0.003	0.162 ± 0.001	1.083 ± 0.003	0.406 ± 0.001	0.3607 ± 0.0009
00	5.4	0.0041 ± 0.0009	0.0029 ± 0.0009	0.854 ± 0.049	1.422 ± 0.015	0.159 ± 0.003	1.370 ± 0.016	0.414 ± 0.008	0.487 ± 0.008
50	5.0	0.0053 ± 0.0009	0.0076 ± 0.0008	0.602 ± 0.034	0.889 ± 0.022	0.139 ± 0.009	0.857 ± 0.089	0.409 ± 0.021	0.363 ± 0.008
	349.6								

Table 4b. Xenon in irradiated Bjurböle for Nadiabondi 1.498 g.

Temp. (°C)	[132] $\times 10^{-12}$ (cm³ STP/g)	$^{124}Xe/^{132}Xe$	$^{126}Xe/^{132}Xe$	$^{128}Xe/^{132}Xe$	$^{129}Xe/^{132}Xe$	$^{130}Xe/^{123}Xe$	$^{131}Xe/^{132}Xe$	$^{134}Xe/^{132}Xe$	$^{136}Xe/^{132}Xe$
Blank	0.033 ± 0.019	0.0082 ± 0.0328	0.0042 ± 0.0049	0.265 ± 1.706	0.728 ± 0.400	0.273 ± 0.159	0.391 ± 0.464		
600	5.0	0.0054 ± 0.0007	0.0062 ± 0.0005	2.700 ± 0.003	1.208 ± 0.014	0.176 ± 0.003	9.68 ± 0.22	0.645 ± 0.009	0.614 ± 0.012
700	4.7	0.0012 ± 0.0010	0.0019 ± 0.0006	2.75 ± 0.66	0.615 ± 0.017	0.0956 ± 0.0040	4.89 ± 0.12	1.043 ± 0.017	1.533 ± 0.039
800	5.7	0.0017 ± 0.0005		6.077 ± 0.026	0.727 ± 0.010	0.0699 ± 0.0024	7.64 ± 0.06	1.193 ± 0.010	1.449 ± 0.068
900	5.9	0.0060 ± 0.0008	0.0060 ± 0.0010	6.619 ± 0.068	1.216 ± 0.014	0.122 ± 0.002	6.835 ± 0.069	0.770 ± 0.013	1.000 ± 0.017
1000	7.5	0.0036 ± 0.0006	0.0040 ± 0.0008	4.707 ± 0.048	1.611 ± 0.018	0.155 ± 0.002	5.95 ± 0.06	0.704 ± 0.012	0.799 ± 0.013
1100	35.0	0.0042 ± 0.0002	0.0040 ± 0.0003	2.534 ± 0.008	1.729 ± 0.009	0.154 ± 0.001	2.41 ± 0.01	0.432 ± 0.005	0.412 ± 0.002
1200	112.8	0.0035 ± 0.0001	0.0035 ± 0.0001	3.048 ± 0.005	2.135 ± 0.006	0.160 ± 0.001	1.594 ± 0.004	0.406 ± 0.001	0.378 ± 0.001
1300	118.3	0.0047 ± 0.0001	0.0042 ± 0.0001	2.003 ± 0.005	1.718 ± 0.005	0.162 ± 0.001	1.144 ± 0.003	0.400 ± 0.002	0.364 ± 0.001
1400	198.6	0.0048 ± 0.0001	0.0043 ± 0.0001	1.011 ± 0.002	1.375 ± 0.002	0.1667 ± 0.0006	0.943 ± 0.002	0.404 ± 0.001	0.3653 ± 0.0009
1500	51.8	0.0042 ± 0.0003	0.0039 ± 0.0004	2.117 ± 0.010	1.854 ± 0.005	0.153 ± 0.003	0.930 ± 0.004	0.426 ± 0.003	0.402 ± 0.001
1600	7.1	0.0058 ± 0.0005	0.0065 ± 0.0016	2.581 ± 0.034	1.866 ± 0.036	0.145 ± 0.004	0.959 ± 0.007	0.444 ± 0.004	0.445 ± 0.007
1650	5.5	0.0033 ± 0.0005	0.0031 ± 0.0006	1.385 ± 0.016	1.189 ± 0.013	0.164 ± 0.005	0.900 ± 0.016	0.429 ± 0.006	0.395 ± 0.006
	557.9								

Table 5a. Xenon in irradiated Beaver Creek (H 4) 1.740 g.

Temp. (°C)	[132] $\times 10^{-12}$ (cm³ STP/g)	$^{124}Xe/^{132}Xe$	$^{126}Xe/^{132}Xe$	$^{128}Xe/^{132}Xe$	$^{129}Xe/^{132}Xe$	$^{130}Xe/^{132}Xe$	$^{131}Xe/^{132}Xe$	$^{134}Xe/^{132}Xe$	$^{136}Xe/^{132}Xe$
Blank	0.017 ± 0.006	0.0110 ± 0.0046	0.943 ± 0.334	3.888 ± 1.032	4.270 ± 2.069	1.092 ± 0.592	3.370 ± 1.361	3.102 ± 1.103	0.723 ± 0.261
600	2.5	0.0008 ± 0.0008	0.0021 ± 0.0007	4.28 ± 0.06	1.16 ± 0.02	0.158 ± 0.004	1.17 ± 0.03	0.347 ± 0.021	0.302 ± 0.014
700	0.2			3.19 ± 0.08	0.72 ± 0.13	0.109 ± 0.040	1.20 ± 0.08	0.599 ± 0.060	0.758 ± 0.077
800	1.2			1.33 ± 0.03	0.359 ± 0.032	0.040 ± 0.009	1.78 ± 0.03	1.412 ± 0.026	1.737 ± 0.031
900	0.5	0.0066 ± 0.0023	0.0054 ± 0.0032	3.21 ± 0.14	1.06 ± 0.06	0.173 ± 0.017	2.76 ± 0.12	0.570 ± 0.033	0.757 ± 0.031
1000	1.1	0.0056 ± 0.0014	0.0089 ± 0.0024	1.70 ± 0.04	1.23 ± 0.02	0.160 ± 0.008	3.42 ± 0.08	0.494 ± 0.012	0.505 ± 0.004
1100	2.9	0.0062 ± 0.0011	0.0073 ± 0.0013	1.00 ± 0.02	1.31 ± 0.02	0.155 ± 0.003	2.46 ± 0.04	0.434 ± 0.013	0.437 ± 0.010
1200	11.6	0.0039 ± 0.0006	0.0062 ± 0.0005	0.622 ± 0.005	1.721 ± 0.016	0.156 ± 0.001	1.901 ± 0.015	0.383 ± 0.005	0.346 ± 0.006

Table 5a (continued).

Temp. °C)	[132] $\times 10^{-12}$ (cm³ STP/g)	$^{124}Xe/^{132}Xe$	$^{126}Xe/^{132}Xe$	$^{128}Xe/^{132}Xe$	$^{129}Xe/^{132}Xe$	$^{130}Xe/^{132}Xe$	$^{131}Xe/^{132}Xe$	$^{134}Xe/^{132}Xe$	$^{136}Xe/^{132}Xe$
300	53.9	0.0038 ± 0.0002	0.0037 ± 0.0002	0.423 ± 0.002	1.512 ± 0.005	0.163 ± 0.001	1.347 ± 0.007	0.391 ± 0.003	0.332 ± 0.003
350	54.5	0.0043 ± 0.0003	0.0040 ± 0.0003	0.410 ± 0.002	1.473 ± 0.007	0.1570 ± 0.0009	1.117 ± 0.005	0.384 ± 0.003	0.326 ± 0.002
400	45.5	0.0106 ± 0.0020	0.0037 ± 0.0005	0.343 ± 0.005	1.403 ± 0.008	0.163 ± 0.003	1.047 ± 0.004	0.388 ± 0.005	0.321 ± 0.003
450	49.5	0.0016 ± 0.0003	0.0034 ± 0.0003	0.379 ± 0.008	1.422 ± 0.015	0.167 ± 0.004	0.937 ± 0.009	0.340 ± 0.008	0.332 ± 0.002
500	46.9	0.0107 ± 0.0024	0.0080 ± 0.0011	0.520 ± 0.005	1.600 ± 0.017	0.176 ± 0.003	0.948 ± 0.008	0.390 ± 0.006	0.338 ± 0.003
600	23.2	0.0023 ± 0.0002	0.0027 ± 0.0003	0.725 ± 0.005	1.792 ± 0.006	0.153 ± 0.003	0.895 ± 0.005	0.389 ± 0.005	0.332 ± 0.003
650	6.1			0.703 ± 0.019	1.824 ± 0.024	0.159 ± 0.012	0.917 ± 0.020	0.403 ± 0.021	0.353 ± 0.018
	299.6								

Table 5b. Xenon in irradiated Bjurböle for Beaver Creek 1.696 g.

Temp. °C)	[132] $\times 10^{-12}$ (cm³ STP/g)	$^{124}Xe/^{132}Xe$	$^{126}Xe/^{132}Xe$	$^{128}Xe/^{132}Xe$	$^{129}Xe/^{132}Xe$	$^{130}Xe/^{132}Xe$	$^{131}Xe/^{132}Xe$	$^{134}Xe/^{132}Xe$	$^{136}Xe/^{132}Xe$
Blank	0.019 ± 0.014			0.420 ± 0.260					0.096 ± 0.238
800	0.5	0.0052 ± 0.0044		1.83 ± 0.09	1.13 ± 0.07	0.106 ± 0.016	2.58 ± 0.11	0.500 ± 0.024	0.520 ± 0.029
900	1.3		0.0043 ± 0.0007	2.55 ± 0.05	1.36 ± 0.03	0.165 ± 0.008	3.51 ± 0.04	0.492 ± 0.012	0.489 ± 0.019
000	26.0	0.0035 ± 0.0004	0.0034 ± 0.0003	1.661 ± 0.005	1.93 ± 0.01	0.149 ± 0.002	2.17 ± 0.02	0.445 ± 0.005	0.415 ± 0.004
100	7.6	0.0028 ± 0.0013	0.0033 ± 0.0012	0.841 ± 0.006	1.49 ± 0.02	0.155 ± 0.004	1.43 ± 0.02	0.433 ± 0.008	0.345 ± 0.005
200	87.9	0.0031 ± 0.0001	0.0034 ± 0.0001	0.846 ± 0.003	1.875 ± 0.008	0.159 ± 0.001	1.102 ± 0.002	0.390 ± 0.002	0.329 ± 0.002
300	145.8	0.0032 ± 0.0001	0.00318 ± 0.00004	0.973 ± 0.002	2.010 ± 0.003	0.1634 ± 0.0005	0.985 ± 0.002	0.391 ± 0.002	0.3354 ± 0.0005
350	102.8	0.00316 ± 0.00008	0.00272 ± 0.00008	0.581 ± 0.003	1.605 ± 0.004	0.160 ± 0.001	0.901 ± 0.002	0.390 ± 0.002	0.331 ± 0.002
400	104.9	0.0035 ± 0.0001	0.0029 ± 0.0001	0.416 ± 0.001	1.428 ± 0.005	0.163 ± 0.001	0.872 ± 0.002	0.385 ± 0.002	0.327 ± 0.002
450	73.6	0.0035 ± 0.0001	0.0027 ± 0.0002	0.428 ± 0.003	1.433 ± 0.004	0.160 ± 0.001	0.849 ± 0.005	0.391 ± 0.002	0.333 ± 0.002
500	79.4	0.0034 ± 0.0002	0.0021 ± 0.0005	0.647 ± 0.006	1.699 ± 0.009	0.155 ± 0.001	0.852 ± 0.006	0.400 ± 0.002	0.344 ± 0.003
600	8.8	0.0199 ± 0.0027	0.0221 ± 0.0062	0.954 ± 0.022	2.012 ± 0.080	0.147 ± 0.007	0.837 ± 0.024	0.474 ± 0.014	0.335 ± 0.005
650	1.2		0.0013 ± 0.0026	0.911 ± 0.021	1.982 ± 0.050	0.133 ± 0.009	0.845 ± 0.023	0.371 ± 0.020	0.315 ± 0.017
	639.8								

Table 6a. Xenon in irradiated Ambapur Nagla (H 5/6)[a] 3.510 g ([a] There is some uncertainty based on feldspar mineralogy as to whether Ambapur Nagla is petrologic type 5 or type 6 [9]).

Temp. (°C)	[132] $\times 10^{-12}$ (cm³ STP/g)	$^{124}Xe/^{132}Xe$	$^{126}Xe/^{132}Xe$	$^{128}Xe/^{132}Xe$	$^{129}Xe/^{132}Xe$	$^{130}Xe/^{132}Xe$	$^{131}Xe/^{132}Xe$	$^{134}Xe/^{132}Xe$	$^{136}Xe/^{132}Xe$
Blank	0.085 ± 0.030	0.3261 ± 0.0758	0.1628 ± 0.0276	0.336 ± 0.057	0.912 ± 0.142	0.648 ± 0.113	0.543 ± 0.146	0.173 ± 0.062	0.449 ± 0.021
600	12.7	0.0035 ± 0.0003	0.0041 ± 0.0003	2.97 ± 0.04	1.308 ± 0.009	0.148 ± 0.002	2.08 ± 0.02	0.416 ± 0.003	0.370 ± 0.003
700	5.4	0.0022 ± 0.0003	0.0029 ± 0.0003	1.230 ± 0.009	0.866 ± 0.009	0.105 ± 0.002	1.80 ± 0.02	0.808 ± 0.005	1.02 ± 0.01
800	2.8	0.0036 ± 0.0004	0.0040 ± 0.0008	2.31 ± 0.05	1.23 ± 0.02	0.137 ± 0.006	2.67 ± 0.06	0.591 ± 0.019	0.573 ±0.020
900	5.6	0.0036 ± 0.0003	0.0047 ± 0.0004	1.180 ± 0.007	1.27 ± 0.01	0.139 ± 0.002	4.23 ± 0.02	0.460 ± 0.006	0.456 ± 0.006
1000	9.2	0.0056 ± 0.0002	0.0051 ± 0.0003	0.694 ± 0.005	1.450 ± 0.008	0.156 ± 0.002	2.86 ± 0.02	0.404 ± 0.004	0.372 ± 0.004
1100	18.3	0.0041 ± 0.0002	0.0044 ± 0.0001	0.456 ± 0.003	1.375 ± 0.008	0.150 ± 0.002	1.76 ± 0.01	0.426 ± 0.001	0.374 ± 0.002
1200	28.7	0.0039 ± 0.0002	0.0039 ± 0.0002	0.402 ± 0.002	1.389 ± 0.006	0.162 ± 0.001	1.385 ± 0.008	0.399 ± 0.002	0.344 ± 0.002
1300	53.0	0.0033 ± 0.0001	0.0032 ± 0.0001	0.382 ± 0.002	1.355 ± 0.006	0.162 ± 0.001	1.113 ± 0.006	0.395 ± 0.002	0.337 ± 0.001
1350	19.0	0.0043 ± 0.0001	0.0039 ± 0.0003	0.526 ± 0.003	1.489 ± 0.009	0.158 ± 0.001	1.038 ± 0.009	0.390 ± 0.002	0.338 ± 0.001
1400	3.7	0.0052 ± 0.0006	0.0048 ± 0.0005	0.616 ± 0.006	1.551 ± 0.014	0.169 ± 0.003	1.07 ± 0.01	0.396 ± 0.005	0.357 ± 0.006
1450	2.9	0.0038 ± 0.0007	0.0036 ± 0.0007	0.643 ± 0.005	1.625 ± 0.012	0.173 ± 0.002	1.031 ± 0.008	0.404 ± 0.007	0.338 ± 0.005
1500	13.6	0.0045 ± 0.0005	0.0032 ± 0.0004	0.684 ± 0.009	1.648 ± 0.009	0.157 ± 0.003	1.01 ± 0.01	0.389 ± 0.007	0.337 ± 0.004
1600	4.8	0.0023 ± 0.0007	0.0025 ± 0.0005	0.650 ± 0.006	1.595 ± 0.017	0.165 ± 0.003	1.00 ± 0.02	0.410 ± 0.006	0.345 ± 0.003
1650	0.4	0.0272 ± 0.0073		0.349 ± 0.076	0.979 ± 0.203	0.082 ± 0.032	0.732 ± 0.140	0.219 ± 0.046	0.370 ± 0.036
	180.1								

Table 6b. Xenon in irradiated Bjurböle for Ambapur Nagla 1.695 g.

Temp. (°C)	[132] $\times 10^{-12}$ (cm³ STP/g)	$^{124}Xe/^{132}Xe$	$^{126}Xe/^{132}Xe$	$^{128}Xe/^{132}Xe$	$^{129}Xe/^{132}Xe$	$^{130}Xe/^{132}Xe$	$^{131}Xe/^{132}Xe$	$^{134}Xe/^{132}Xe$	$^{136}Xe/^{132}Xe$
Blank	0.019 ± 0.013			0.288 ± 0.073	1.04 ± 0.18	0.178 ± 0.059	0.863 ± 0.033	0.384 ± 0.025	0.329 ± 0.036
600	5.6	0.0239 ± 0.0053	0.0707 ± 0.0208	1.05 ± 0.24	1.34 ± 0.02	0.153 ± 0.002	5.09 ± 0.14	0.410 ± 0.003	0.426 ± 0.007
700	4.8	0.0195 ± 0.0052	0.0453 ± 0.0153	1.95 ± 0.01	0.759 ± 0.011	0.096 ± 0.003	3.99 ± 0.07	0.992 ± 0.013	1.187 ± 0.016
800	7.5	0.0408 ± 0.0088	0.0183 ± 0.0040	1.45 ± 0.19	1.45 ± 0.02	0.147 ± 0.003	4.03 ± 0.05	0.493 ± 0.008	0.495 ± 0.008
900	10.0	0.0033 ± 0.0005	0.0033 ± 0.0008	2.30 ± 0.04	1.76 ± 0.03	0.147 ± 0.003	1.72 ± 0.10	0.444 ± 0.008	0.428 ± 0.002
1000	21.3	0.0047 ± 0.0007	0.0033 ± 0.0007	1.38 ± 0.01	1.55 ± 0.05	0.158 ± 0.003	1.50 ± 0.01	0.396 ± 0.009	0.358 ± 0.006

Table 6b (continued).

Temp. °C)	[132] $\times 10^{-12}$ (cm³ STP/g)	$^{124}Xe/^{132}Xe$	$^{126}Xe/^{132}Xe$	$^{128}Xe/^{132}Xe$	$^{129}Xe/^{132}Xe$	$^{130}Xe/^{132}Xe$	$^{131}Xe/^{132}Xe$	$^{134}Xe/^{132}Xe$	$^{136}Xe/^{132}Xe$
100	138.0	0.0040 ± 0.0001	0.0036 ± 0.0001	1.046 ± 0.002	2.099 ± 0.003	0.166 ± 0.001	1.079 ± 0.004	0.395 ± 0.001	0.334 ± 0.001
200	171.7	0.00373 ± 0.00009	0.00332 ± 0.00008	0.621 ± 0.001	1.631 ± 0.002	0.1633 ± 0.0005	0.903 ± 0.003	0.390 ± 0.001	0.3313 ± 0.0005
300	143.4	0.00367 ± 0.00008	0.00330 ± 0.00004	0.463 ± 0.002	1.479 ± 0.003	0.1633 ± 0.0008	0.865 ± 0.003	0.388 ± 0.001	0.330 ± 0.002
350	17.9	0.0025 ± 0.0003	0.0028 ± 0.0003	0.819 ± 0.005	1.854 ± 0.014	0.150 ± 0.002	0.875 ± 0.007	0.383 ± 0.003	0.335 ± 0.003
400	11.7	0.0029 ± 0.0002	0.0029 ± 0.0003	0.964 ± 0.009	2.05 ± 0.02	0.157 ± 0.002	0.845 ± 0.008	0.386 ± 0.007	0.354 ± 0.004
450	17.7	0.0030 ± 0.0003	0.0034 ± 0.0003	1.033 ± 0.002	2.13 ± 0.01	0.156 ± 0.002	0.853 ± 0.009	0.393 ± 0.004	0.339 ± 0.001
500	8.9	0.0032 ± 0.0004	0.0033 ± 0.0003	0.993 ± 0.008	2.09 ± 0.02	0.149 ± 0.003	0.829 ± 0.011	0.385 ± 0.005	0.340 ± 0.004
600	0.9	0.0290 ± 0.0052	0.0571 ± 0.0076	0.920 ± 0.028	2.05 ± 0.06	0.250 ± 0.011	1.22 ± 0.05	0.433 ± 0.008	0.282 ± 0.012
650	0.5	0.0686 ± 0.0159	0.1108 ± 0.0321	0.238 ± 0.027	1.26 ± 0.04	0.144 ± 0.016	0.833 ± 0.051	0.450 ± 0.016	0.152 ± 0.032
	559.9								

Table 7a. Xenon in irradiated Kernouve (H 6) 4.191 g.

Temp. °C)	[132] $\times 10^{-12}$ (cm³ STP/g)	$^{124}Xe/^{132}Xe$	$^{126}Xe/^{132}Xe$	$^{128}Xe/^{132}Xe$	$^{129}Xe/^{132}Xe$	$^{130}Xe/^{132}Xe$	$^{131}Xe/^{132}Xe$	$^{134}Xe/^{132}Xe$	$^{136}Xe/^{132}Xe$
Blank	0.21 ± 0.01	0.0062 ± 0.0024		0.770 ± 0.047	1.639 ± 0.028	0.129 ± 0.018	0.866 ± 0.038	0.385 ± 0.024	0.276 ± 0.034
600	2.3	0.0019 ± 0.0005	0.0019 ± 0.0007	41.45 ± 0.24	1.027 ± 0.006	0.148 ± 0.005	6.12 ± 0.04	0.419 ± 0.008	0.377 ± 0.005
700	2.6			3.12 ± 0.02	0.418 ± 0.011	0.055 ± 0.003	3.24 ± 0.02	1.339 ± 0.013	1.779 ± 0.013
800	3.8	0.0022 ± 0.0002	0.0019 ± 0.0004	2.51 ± 0.02	0.963 ± 0.007	0.138 ± 0.003	2.06 ± 0.02	0.482 ± 0.003	0.482 ± 0.006
900	1.7	0.0022 ± 0.0006	0.0031 ± 0.0004	2.09 ± 0.01	0.987 ± 0.013	0.138 ± 0.005	2.13 ± 0.02	0.486 ± 0.006	0.459 ± 0.008
1000	5.3	0.0020 ± 0.0003	0.0023 ± 0.0004	1.19 ± 0.01	1.029 ± 0.009	0.1453 ± 0.0008	1.694 ± 0.007	0.427 ± 0.005	0.379 ± 0.005
1100	3.2	0.0029 ± 0.0005	0.0025 ± 0.0005	0.906 ± 0.010	1.122 ± 0.010	0.139 ± 0.008	2.30 ± 0.01	0.446 ± 0.003	0.426 ± 0.004
1200	6.4	0.0034 ± 0.0002	0.0027 ± 0.0003	0.491 ± 0.003	1.123 ± 0.006	0.138 ± 0.001	3.33 ± 0.01	0.533 ± 0.004	0.528 ± 0.005
1300	7.7	0.0033 ± 0.0002	0.0034 ± 0.0006	0.262 ± 0.003	1.288 ± 0.008	0.146 ± 0.003	3.08 ± 0.01	0.464 ± 0.002	0.444 ± 0.005
1350	15.6	0.0028 ± 0.0002	0.00333 ± 0.00006	0.196 ± 0.002	1.231 ± 0.006	0.153 ± 0.002	1.689 ± 0.006	0.410 ± 0.002	0.362 ± 0.003
1400	9.1	0.0030 ± 0.0003	0.0028 ± 0.0003	0.157 ± 0.002	1.184 ± 0.007	0.157 ± 0.002	1.186 ± 0.007	0.391 ± 0.002	0.328 ± 0.004
1450	15.5	0.0038 ± 0.0004	0.0046 ± 0.0004	0.186 ± 0.003	1.249 ± 0.007	0.154 ± 0.002	1.012 ± 0.006	0.394 ± 0.003	0.336 ± 0.004
1500	13.0	0.0038 ± 0.0004	0.0041 ± 0.0005	0.196 ± 0.003	1.266 ± 0.011	0.1556 ± 0.0006	0.964 ± 0.006	0.386 ± 0.005	0.336 ± 0.001
1600	8.0	0.0034 ± 0.0005	0.0039 ± 0.0006	0.272 ± 0.003	1.416 ± 0.020	0.169 ± 0.003	0.960 ± 0.013	0.372 ± 0.008	0.322 ± 0.004
1650	1.9			0.263 ± 0.012	1.46 ± 0.09	0.156 ± 0.012	0.931 ± 0.054	0.400 ± 0.037	0.335 ± 0.028
	96.1								

Table 7b. Xenon in irradiated Bjurböle for Kernouve 1.787 g.

Temp. (°C)	[132] $\times 10^{-12}$ (cm³ STP/g)	$^{124}Xe/^{132}Xe$	$^{126}Xe/^{132}Xe$	$^{128}Xe/^{132}Xe$	$^{129}Xe/^{132}Xe$	$^{130}Xe/^{132}Xe$	$^{131}Xe/^{132}Xe$	$^{134}Xe/^{132}Xe$	$^{136}Xe/^{132}Xe$
Blank	0.12 ± 0.01	0.0132 ± 0.0234			1.869 ± 0.094	0.073 ± 0.035	0.382 ± 0.072	0.207 ± 0.059	0.215 ± 0.037
800	1.6			2.69 ± 0.15	1.105 ± 0.040	0.139 ± 0.013	3.75 ± 0.16	0.778 ± 0.051	0.935 ± 0.063
900	4.9	0.0042 ± 0.0013	0.0040 ± 0.0015	1.827 ± 0.019	1.381 ± 0.014	0.154 ± 0.007	3.02 ± 0.07	0.535 ± 0.011	0.524 ± 0.013
1000	4.9	0.0038 ± 0.0010	0.0036 ± 0.0012	1.802 ± 0.023	1.506 ± 0.018	0.146 ± 0.005	2.97 ± 0.05	0.471 ± 0.008	0.460 ± 0.007
1100	10.2	0.0030 ± 0.0003	0.0025 ± 0.0004	1.197 ± 0.010	1.674 ± 0.011	0.151 ± 0.002	1.85 ± 0.02	0.407 ± 0.004	0.394 ± 0.002
1200	149.8	0.0035 ± 0.0001	0.00318 ± 0.00007	0.975 ± 0.002	2.038 ± 0.004	0.1603 ± 0.0009	1.105 ± 0.002	0.398 ± 0.001	0.340 ± 0.001
1300	135.7	0.0034 ± 0.0001	0.0031 ± 0.0001	0.6169 ± 0.0005	1.650 ± 0.003	0.162 ± 0.001	0.919 ± 0.002	0.3943 ± 0.0007	0.337 ± 0.002
1350	90.7	0.0034 ± 0.0002	0.00344 ± 0.00003	0.436 ± 0.002	1.461 ± 0.005	0.164 ± 0.001	0.866 ± 0.003	0.391 ± 0.002	0.332 ± 0.001
1400	57.1	0.0032 ± 0.0002	0.0028 ± 0.0001	0.480 ± 0.002	1.537 ± 0.005	0.166 ± 0.001	0.858 ± 0.003	0.397 ± 0.002	0.335 ± 0.002
1450	27.9	0.0025 ± 0.0002	0.0025 ± 0.0003	0.672 ± 0.005	1.773 ± 0.011	0.157 ± 0.001	0.871 ± 0.004	0.399 ± 0.003	0.351 ± 0.002
1500	13.0	0.0029 ± 0.0008	0.0039 ± 0.0006	0.800 ± 0.022	1.920 ± 0.021	0.148 ± 0.003	0.823 ± 0.017	0.381 ± 0.008	0.358 ± 0.005
1600	3.3	0.0006 ± 0.0010	0.0021 ± 0.0005	0.721 ± 0.012	1.812 ± 0.012	0.148 ± 0.005	0.764 ± 0.013	0.376 ± 0.009	0.331 ± 0.005
1650	7.4			0.917 ± 0.008	2.115 ± 0.007	0.161 ± 0.003	0.861 ± 0.007	0.398 ± 0.006	0.343 ± 0.005
	506.5								

Table 8a. Xenon in irradiated Ausson (L 5) 2.241 g.

Temp. (°C)	[132] $\times 10^{-12}$ (cm³ STP/g)	$^{124}Xe/^{132}Xe$	$^{126}Xe/^{132}Xe$	$^{128}Xe/^{132}Xe$	$^{129}Xe/^{132}Xe$	$^{130}Xe/^{132}Xe$	$^{132}Xe/^{132}Xe$	$^{134}Xe/^{132}Xe$	$^{136}Xe/^{132}Xe$
Blank	0.030 ± 0.017	0.0763 ± 0.0265	0.1293 ± 0.0315	0.480 ± 0.238	0.936 ± 0.300	0.276 ± 0.048	0.677 ± 0.132		0.451 ± 0.044
600	3.8	0.0037 ± 0.0007	0.0033 ± 0.0005	7.39 ± 0.06	1.21 ± 0.02	0.151 ± 0.007	4.36 ± 0.06	0.427 ± 0.006	0.388 ± 0.010
700	4.4	0.0019 ± 0.0006	0.0046 ± 0.0006	0.723 ± 0.009	0.688 ± 0.015	0.084 ± 0.003	3.49 ± 0.03	0.995 ± 0.011	1.249 ± 0.008
800	4.4	0.0053 ± 0.0008	0.0075 ± 0.0008	0.574 ± 0.006	1.13 ± 0.02	0.144 ± 0.005	3.07 ± 0.04	0.505 ± 0.003	0.506 ± 0.008
900	4.8	0.0072 ± 0.0006	0.0102 ± 0.0010	0.399 ± 0.008	1.15 ± 0.01	0.159 ± 0.011	3.16 ± 0.03	0.435 ± 0.009	0.411 ± 0.005
1000	6.6	0.0079 ± 0.0007	0.0106 ± 0.0008	0.366 ± 0.006	1.23 ± 0.01	0.153 ± 0.004	3.05 ± 0.03	0.433 ± 0.007	0.392 ± 0.006
1100	9.5	0.0078 ± 0.0007	0.0103 ± 0.0006	0.384 ± 0.004	1.40 ± 0.01	0.168 ± 0.004	2.56 ± 0.02	0.410 ± 0.006	0.358 ± 0.006
1200	14.8	0.0062 ± 0.0005	0.0076 ± 0.0003	0.384 ± 0.002	1.443 ± 0.008	0.153 ± 0.003	1.74 ± 0.01	0.413 ± 0.005	0.381 ± 0.004
1300	44.6	0.0046 ± 0.0001	0.00521 ± 0.00007	0.342 ± 0.002	1.391 ± 0.007	0.1632 ± 0.0009	1.204 ± 0.004	0.401 ± 0.002	0.348 ± 0.002

Table 8a (continued).

Temp. (°C)	[132] $\times 10^{-12}$ (cm³ STP/g)	$^{124}Xe/^{132}Xe$	$^{126}Xe/^{132}Xe$	$^{128}Xe/^{132}Xe$	$^{129}Xe/^{132}Xe$	$^{130}Xe/^{132}Xe$	$^{131}Xe/^{132}Xe$	$^{134}Xe/^{132}Xe$	$^{136}Xe/^{132}Xe$
1350	32.9	0.0032 ± 0.0002	0.0043 ± 0.0003	0.530 ± 0.003	1.648 ± 0.004	0.1584 ± 0.0009	1.075 ± 0.005	0.393 ± 0.003	0.348 ± 0.002
1400	7.0	0.0032 ± 0.0004	0.0027 ± 0.0004	0.537 ± 0.006	1.702 ± 0.015	0.1564 ± 0.0009	1.01 ± 0.01	0.387 ± 0.006	0.340 ± 0.006
1450	3.9	0.0030 ± 0.0005	0.0025 ± 0.0005	0.482 ± 0.010	1.705 ± 0.009	0.155 ± 0.005	0.979 ± 0.019	0.404 ± 0.009	0.354 ± 0.008
1500	1.2	0.0020 ± 0.0013	0.0025 ± 0.0013	0.415 ± 0.017	1.53 ± 0.02	0.170 ± 0.009	0.985 ± 0.015	0.386 ± 0.007	0.330 ± 0.006
1600	4.2	0.0038 ± 0.0010	0.0039 ± 0.0009	0.437 ± 0.013	1.525 ± 0.015	0.173 ± 0.009	0.947 ± 0.015	0.381 ± 0.008	0.343 ± 0.010
1650	0.3	0.0061 ± 0.0022	0.0104 ± 0.0039	0.356 ± 0.024	1.338 ± 0.050	0.141 ± 0.012	0.814 ± 0.053	0.456 ± 0.029	0.306 ± 0.030
	142.4								

Table 8b. Xenon in irradiated Bjurböle for Ausson 1.808 g.

Temp. (°C)	[132] $\times 10^{-12}$ (cm³ STP/g)	$^{124}Xe/^{132}Xe$	$^{126}Xe/^{132}Xe$	$^{128}Xe/^{132}Xe$	$^{129}Xe/^{132}Xe$	$^{130}Xe/^{132}Xe$	$^{131}Xe/^{132}Xe$	$^{134}Xe/^{132}Xe$	$^{136}Xe/^{132}Xe$
Blank	0.026 ± 0.017		0.0538 ± 0.0099		1.189 ± 0.213	0.210 ± 0.019	0.802 ± 0.204		0.036 ± 0.092
600	7.2	0.0027 ± 0.0005	0.0029 ± 0.0004	8.32 ± 0.06	1.29 ± 0.01	0.156 ± 0.005	3.40 ± 0.04	0.399 ± 0.007	0.352 ± 0.005
700	4.0	0.0005 ± 0.0010	0.0003 ± 0.0010	2.27 ± 0.02	0.786 ± 0.015	0.095 ± 0.004	4.72 ± 0.04	1.02 ± 0.01	1.27 ± 0.01
800	4.7	0.0037 ± 0.0006	0.0027 ± 0.0006	3.31 ± 0.05	1.42 ± 0.03	0.133 ± 0.004	4.89 ± 0.09	0.593 ± 0.009	0.635 ± 0.009
900	5.1	0.0038 ± 0.0006	0.0036 ± 0.0007	2.29 ± 0.04	1.68 ± 0.04	0.161 ± 0.005	3.58 ± 0.07	0.467 ± 0.007	0.453 ± 0.006
1000	12.1	0.0035 ± 0.0005	0.0027 ± 0.0006	1.48 ± 0.01	1.86 ± 0.01	0.159 ± 0.003	2.10 ± 0.02	0.416 ± 0.005	0.372 ± 0.007
1100	75.9	0.0034 ± 0.0003	0.0028 ± 0.0004	0.783 ± 0.003	1.829 ± 0.009	0.164 ± 0.002	1.138 ± 0.005	0.383 ± 0.004	0.329 ± 0.005
1200	159.9	0.0035 ± 0.0002	0.0033 ± 0.0005	1.002 ± 0.002	2.157 ± 0.005	0.1617 ± 0.0008	1.004 ± 0.002	0.388 ± 0.002	0.328 ± 0.002
1300	150.2	0.0029 ± 0.0001	0.0029 ± 0.0001	0.485 ± 0.002	1.539 ± 0.003	0.1626 ± 0.0009	0.885 ± 0.002	0.387 ± 0.001	0.3271 ± 0.0008
1350	142.6	0.00351 ± 0.00009	0.0033 ± 0.0001	0.367 ± 0.002	1.411 ± 0.005	0.164 ± 0.001	0.859 ± 0.002	0.380 ± 0.001	0.323 ± 0.001
1400	51.1	0.0033 ± 0.0002	0.0028 ± 0.0002	0.544 ± 0.004	1.670 ± 0.007	0.159 ± 0.002	0.854 ± 0.006	0.392 ± 0.003	0.342 ± 0.003
1450	18.2	0.0027 ± 0.0004	0.0021 ± 0.0003	0.830 ± 0.009	1.990 ± 0.012	0.149 ± 0.001	0.863 ± 0.010	0.391 ± 0.005	0.331 ± 0.003
1500	14.3	0.0037 ± 0.0005	0.0022 ± 0.0003	1.086 ± 0.009	2.286 ± 0.015	0.155 ± 0.002	0.856 ± 0.007	0.386 ± 0.008	0.341 ± 0.005
1600	8.2	0.0032 ± 0.0006		1.113 ± 0.035	2.324 ± 0.047	0.163 ± 0.005	0.840 ± 0.016	0.421 ± 0.009	0.327 ± 0.008
1650	1.4		0.0023 ± 0.0017	0.673 ± 0.022	1.909 ± 0.040	0.178 ± 0.010	0.839 ± 0.027	0.370 ± 0.008	0.336 ± 0.011
	654.9								

Table 9a. Xenon in irradiated Peetz (L 6) 4.564 g.

Temp. (°C)	[132] $\times 10^{-12}$ (cm³ STP/g)	$^{124}Xe/^{132}Xe$	$^{126}Xe/^{132}Xe$	$^{128}Xe/^{132}Xe$	$^{129}Xe/^{132}Xe$	$^{130}Xe/^{132}Xe$	$^{131}Xe/^{132}Xe$	$^{134}Xe/^{132}Xe$	$^{136}Xe/^{132}Xe$
Blank	0.033 ± 0.007	0.0169 ± 0.0044	0.0234 ± 0.0027	1.287 ± 0.516	1.70 ± 0.09	0.160 ± 0.010	1.06 ± 0.06	0.494 ± 0.022	0.271 ± 0.010
600	4.6	0.0033 ± 0.0003	0.0039 ± 0.0004	8.97 ± 0.20	1.301 ± 0.009	0.158 ± 0.002	4.09 ± 0.07	0.403 ± 0.004	0.349 ± 0.004
700	1.3	0.0123 ± 0.0029	0.0159 ± 0.0027	1.12 ± 0.24	1.24 ± 0.04	0.219 ± 0.015	1.02 ± 0.24	0.506 ± 0.023	0.426 ± 0.036
800	1.0	0.0045 ± 0.0009	0.0076 ± 0.0009	5.71 ± 0.13	0.899 ± 0.033	0.118 ± 0.006	6.51 ± 0.14	0.756 ± 0.013	0.866 ± 0.018
900	1.1	0.0066 ± 0.0012	0.0114 ± 0.0012	9.14 ± 0.11	0.895 ± 0.016	0.115 ± 0.004	9.28 ± 0.14	0.704 ± 0.013	0.739 ± 0.017
1000	1.4	0.0112 ± 0.0015	0.0189 ± 0.0014	8.02 ± 0.11	0.965 ± 0.017	0.149 ± 0.006	8.94 ± 0.11	0.603 ± 0.014	0.675 ± 0.009
1100	4.5	0.0132 ± 0.0009	0.0193 ± 0.0007	2.46 ± 0.04	1.146 ± 0.011	0.158 ± 0.002	5.83 ± 0.08	0.541 ± 0.011	0.586 ± 0.010
1200	7.3	0.0095 ± 0.0004	0.0128 ± 0.0007	0.541 ± 0.005	1.049 ± 0.011	0.143 ± 0.003	3.06 ± 0.03	0.546 ± 0.008	0.545 ± 0.008
1250	9.2	0.0047 ± 0.0004	0.0065 ± 0.0006	0.227 ± 0.001	1.151 ± 0.009	0.160 ± 0.002	1.81 ± 0.02	0.441 ± 0.003	0.410 ± 0.005
1300	21.0	0.0050 ± 0.0001	0.0050 ± 0.0002	0.159 ± 0.001	1.117 ± 0.003	0.157 ± 0.001	1.35 ± 0.01	0.396 ± 0.002	0.353 ± 0.002
1350	29.2	0.0045 ± 0.0002	0.0043 ± 0.0001	0.136 ± 0.001	1.102 ± 0.005	0.161 ± 0.002	1.084 ± 0.005	0.384 ± 0.002	0.332 ± 0.002
1400	32.2	0.0039 ± 0.0002	0.0044 ± 0.0001	0.147 ± 0.001	1.142 ± 0.006	0.161 ± 0.001	0.986 ± 0.004	0.387 ± 0.002	0.327 ± 0.002
1500	27.6	0.0042 ± 0.0004	0.0036 ± 0.0003	0.197 ± 0.002	1.215 ± 0.013	0.156 ± 0.003	0.917 ± 0.005	0.379 ± 0.002	0.315 ± 0.002
1600	5.9	0.0039 ± 0.0007	0.0039 ± 0.0006	0.189 ± 0.002	1.195 ± 0.017	0.159 ± 0.004	0.844 ± 0.004	0.377 ± 0.002	0.320 ± 0.003
1650	0.4			0.209 ± 0.030	1.12 ± 0.21	0.158 ± 0.033	0.969 ± 0.061	0.378 ± 0.027	0.337 ± 0.032
	146.7								

are recorded as the first rows in Tables 3a, b to Tables 9a, b. The blank for the low temperature fractions up to ~ 1100 °C is always negligible. The 1200 °C—1400 °C blanks are somewhat lower than the 1500 °C blank, but even if one overcorrects these fractions by subtracting the full 1500 °C blank, there is no essential change in the isotope systematics. In either case ^{129}Xe and ^{128}Xe are generally uncorrelated in all low (up to ~ 1100 °C) temperature fractions. Blank corrections for 1500 °C and 1600 °C are nearly identical due to the shorter (20 minute) extraction time at 1600 °C as compared to the 40 minute 1500 °C extraction. In all cases, but in particular for the most important fractions from 1100 °C to 1500 °C, are these corrections very small or negligible (Tables 12—18). In some cases the 1650 °C fractions were ignored in the fitting routine because of their departures from the correlation line established by the other temperature fractions. These departures were not considered real in the sense that they represent variations in the meteorite composition, but more likely due to under- (or over-) corrections at 1650 °C. This is illustrated for a few 1650 °C fractions in Figs. 5, 7 and 10. The percentage blank at ^{132}Xe for the higher temperature fractions are given in Tables 12—18.

b) Spallation Corrections

After blank subtraction the isotopes ^{124}Xe, ^{126}Xe, and ^{130}Xe are a mixture of spallation products and trapped gas. Spallation composition is traditionally determined as described by Podosek [2] by plotting ($^{126}Xe/^{130}Xe$) vs. ($^{124}Xe/^{130}Xe$) for the different

Table 9b. Xenon in irradiated Bjurböle for Peetz 1.727 g.

Temp. (°C)	[132] $\times 10^{-12}$ (cm^3 STP/g)	$^{124}Xe/^{132}Xe$	$^{126}Xe/^{132}Xe$	$^{128}Xe/^{132}Xe$	$^{129}Xe/^{132}Xe$	$^{130}Xe/^{132}Xe$	$^{131}Xe/^{132}Xe$	$^{134}Xe/^{132}Xe$	$^{136}Xe/^{132}Xe$
Blank	0.38 ± 0.04	0.0386 ± 0.0090	0.0952 ± 0.0214		0.884 ± 0.039	0.130 ± 0.020	0.706 ± 0.064	0.224 ± 0.046	0.366 ± 0.020
600	9.1	0.0053 ± 0.0010	0.0064 ± 0.0007	4.362 ± 0.036	1.160 ± 0.012	0.150 ± 0.002	2.511 ± 0.034	0.410 ± 0.007	0.357 ± 0.005
700	1.4	0.0020 ± 0.0006	0.0019 ± 0.0007	1.68 ± 0.09	1.07 ± 0.03	0.138 ± 0.010	2.36 ± 0.10	0.483 ± 0.034	0.456 ± 0.036
800	4.2	0.0010 ± 0.0007	0.0027 ± 0.0006	2.096 ± 0.039	0.986 ± 0.014	0.113 ± 0.003	3.53 ± 0.07	0.720 ± 0.010	0.886 ± 0.011
900	4.2	0.0062 ± 0.0009	0.0061 ± 0.0008	1.651 ± 0.041	1.314 ± 0.015	0.143 ± 0.003	2.21 ± 0.04	0.469 ± 0.006	0.402 ± 0.005
000	5.2	0.0024 ± 0.0010	0.0015 ± 0.0007	1.716 ± 0.019	1.539 ± 0.017	0.157 ± 0.003	2.582 ± 0.026	0.445 ± 0.007	0.402 ± 0.005
100	44.3	0.0038 ± 0.0003	0.0045 ± 0.0002	1.076 ± 0.004	1.885 ± 0.007	0.156 ± 0.002	1.413 ± 0.006	0.401 ± 0.002	0.350 ± 0.002
200	128.1	0.0040 ± 0.0001	0.0038 ± 0.0001	0.825 ± 0.007	1.988 ± 0.001	0.163 ± 0.005	0.997 ± 0.005	0.389 ± 0.002	0.331 ± 0.001
250	79.0	0.0046 ± 0.0002	0.0043 ± 0.0003	0.769 ± 0.003	1.877 ± 0.005	0.162 ± 0.002	0.924 ± 0.004	0.387 ± 0.003	0.331 ± 0.003
300	83.1	0.0044 ± 0.0001	0.0042 ± 0.0003	0.583 ± 0.002	1.671 ± 0.004	0.1605 ± 0.0008	0.906 ± 0.003	0.394 ± 0.002	0.337 ± 0.002
350	64.9	0.0043 ± 0.0002	0.0039 ± 0.0001	0.392 ± 0.002	1.448 ± 0.004	0.1657 ± 0.0005	0.867 ± 0.004	0.392 ± 0.002	0.332 ± 0.002
400	57.3	0.0040 ± 0.0002	0.0034 ± 0.0002	0.384 ± 0.002	1.438 ± 0.007	0.1574 ± 0.0009	0.855 ± 0.007	0.386 ± 0.003	0.323 ± 0.003
500	50.5	0.0039 ± 0.0002	0.0041 ± 0.0002	0.656 ± 0.002	1.819 ± 0.007	0.159 ± 0.002	0.868 ± 0.005	0.403 ± 0.002	0.352 ± 0.002
600	9.1	0.0039 ± 0.0007	0.0035 ±0.0004	0.852 ± 0.007	2.107 ± 0.022	0.163 ± 0.002	0.864 ± 0.012	0.402 ± 0.007	0.354 ± 0.005
650	2.1	0.0158 ± 0.0046	0.0178 ± 0.0046	0.848 ± 0.038	2.153 ± 0.062	0.179 ± 0.010	0.902 ± 0.039	0.449 ± 0.021	0.337 ± 0.018
	542.5								

temperature fractions with the two component assumption of spallation and trapped gas. Should a simple two component assumption be correct the temperature fractions should fall along a straight line connecting the components, the slope of which gives the $(^{124}Xe/^{126}Xe)_{sp}$ (sp = spallation) ratio. Such a correlation diagram is shown for Peetz in Fig. 2, the xenon of which may be regarded as being composed of a trapped component (in this case it most closely resembles atmosphere) and a single spallation component having a $(^{124}Xe/^{126}Xe)_{sp}$ ratio equal to 0.61 ± 0.07. These ratios as well as the total quantities of extracted $^{126}Xe_{sp}$ are summarized in Table 10. It is noteworthy that, after a large number of measurements, we were able to extract from Bjurböle, in which the trapped component normally dominates, a spallation composition of $(^{124}Xe/^{126}Xe)_{sp} = 0.54 \pm 0.07$ from the lowest (600 °C–800 °C) and highest (1600 °C to 1650 °C) temperature fractions.

As useful as these data might be, it should be emphasized that our main concern was to correct the $^{128}Xe/^{132}Xe$ and $^{129}Xe/^{132}Xe$ ratios for spallation. To this end we have made spallation corrections, in a manner similar to Podosek [2], by partitioning of the $(^{130}Xe/^{126}Xe)$ ratio between a trapped ratio of $(^{130}Xe/^{126}Xe)_t = 41.7 \pm 4.5$ (an average of the extreme values observed in the trapped ratio, atmospheric and SUCOR, both values of which are included in the range) and a spallation ratio of $(^{130}Xe/^{126}Xe)_{sp} = 1.0 \pm 0.2$. Corrections were then applied to the $^{128}Xe/^{132}Xe$ and $^{129}Xe/^{132}Xe$ ratios assuming $(^{132}Xe/^{126}Xe)_{sp} = 1.0$ and $(^{128}Xe/^{126}Xe)_{sp} = 1.5 \pm 0.25$ and $(^{129}Xe/^{126}Xe)_{sp}$

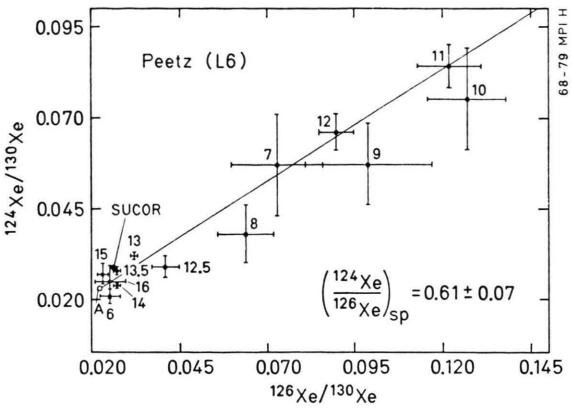

Fig. 2. Spallation diagram for Peetz (L 6). Numbers represent temperature fractions in °C and should be multiplied by 100. The best fit of all data indicate that atmosphere (A) is the most dominant trapped component, although the presence of solar type xenon, represented by Sucor [15] is obvious.

$= 1.25 \pm 0.75$. The adopted ratios fall in the range of meteoritic observations and calculations based on spallation systematics [16, 17, 18, 19, 20]. The percentages of spallation at ^{132}Xe for the higher temperature fractions are given in Tables 12–18. The respective corrections are generally very small.

c) Fission Corrections

After blank and spallation corrections, the system $^{130}Xe/^{132}Xe$, $^{134}Xe/^{132}Xe$, and $^{136}Xe/^{132}Xe$ is composed of a mixture of trapped gas at all isotopes and fission gas at ^{132}Xe, ^{134}Xe and ^{136}Xe. The standard plot of $^{130}Xe/^{132}Xe$ vs. $^{134}Xe/^{132}Xe$ (or $^{136}Xe/^{132}Xe$) can be considered to reflect a mixture of a trapped component and various kinds of fission which plot along the $^{134}Xe/^{132}Xe$ axis where $^{130}Xe/^{132}Xe = 0$ [2]. This plot is illustrated in Fig. 3 by the Bjurböle standard for Nadiabondi which received the highest neutron flux. Provided that the released gases result from a uniform mixture between a trapped component and single or combined fission component, a straight line should be defined in which the fission composition is determined where $^{130}Xe/^{132}Xe = 0$. As seen in Fig. 3, a choice of BEOC 12 [21] for a trapped component with the highest observed $^{130}Xe/^{132}Xe$ and lowest observed $^{134}Xe/^{132}Xe$ ($^{130}Xe/^{132}Xe = 0.165$, $^{134}Xe/^{132}Xe = 0.369$) seems to satisfy most temperature fractions, although choosing a Murray composition ($^{130}Xe/^{132}Xe = 0.162$, $^{134}Xe/^{132}Xe =$

Table 10. Spallation data.

Meteorite	$(^{124}Xe/^{126}Xe)_{sp}$ [a]	$[^{126}Xe_{sp}] \times 10^{-12}$ cm³ STP/g[b]
Menow (H 4)	0.5 ± 0.2	0.2
Nadiabondi (H 5)	0.5 ± 0.1	0.2
Beaver Creek (H 4)	0.5 ± 0.2	0.2
Ambapur Nagla (H 5/6)	too little spallation to determine ratio	0.05
Kernouve (H 6)	too little spallation to determine ratio	0.02
Ausson (L 5)	0.69 ± 0.09	0.3
Peetz (L 6)	0.61 ± 0.07	0.3
Bjurböle (L 4) average [c]	0.54 ± 0.07	0.3 (0–0.8)

[a] Spallation ratio was determined from slope of line defined by temperature fractions in a $^{126}Xe/^{130}Xe$ vs. $^{124}Xe/^{130}Xe$ spallation diagram.

[b] Assumes $(^{130}Xe/^{126}Xe)_{sp} = 1.0$.

[c] Spallation ratio was determined using all Bjurböle standards from temperature fractions with greater than 30% spallation at ^{126}Xe. Up to 99% spallation at this isotope was observed. Spallation yields were highly variable. Two standards showed practically no spallation: One (for Kernouve) was preheated at 800 °C for 2 hours, and the other (for Ausson) had an apparently large trapped component. Two standards (for Menow and Ambapur Nagla) have relatively high spallation yields (0.7, 0.8×10^{-12} cm³ STP/g) at the lowest (600° to 800 °C) and highest (1600°–1650 °C) temperature fractions. The remainder had $(0.1–0.2) \times 10^{-12}$ cm³ STP/g $^{126}Xe_{sp}$.

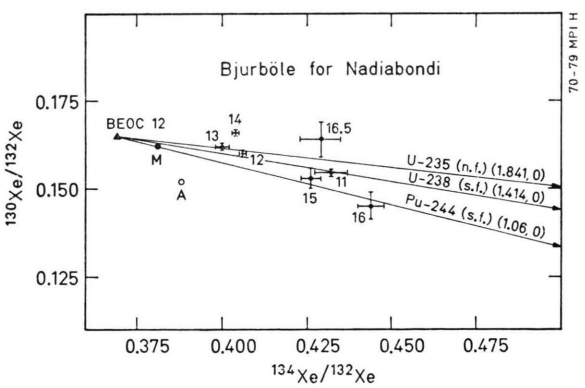

Fig. 3. Three-isotopefission + trapped gas diagram for the n-irradiated Bjurböle standard for Nadiabondi. After spallation corrections, the data should be a mixture of trapped gas and fission components, the compositions of which are defined where $^{130}Xe/^{132}Xe = 0$, since there is no ^{130}Xe in the fission component. These components include neutron induced fission (n. f.), from ^{235}U and spontaneous fission (s. f.) from ^{238}U and ^{244}Pu. Most data fall within a field formed by the solar type trapped value of BEOC 12 [21] or a typical carbonaceous chondrite value like the Murray (M) composition [15] and the various fission components.

Table 11. Fission data.

Irradiation	Meteorite	$(^{134}Xe/^{132}Xe)_{total}$	$(^{132}Xe_f/^{132}Xe)_{total}$ [a]	$[^{132}Xe_f]$ $\times 10^{-12}$ cm^3 STP/g [a]
K-1	Menow (H 4)	0.405	0.025	15.5 ± 4.2
	Nadiabondi (H 5)	0.414	0.033	11.6 ± 3.1
K-2	Beaver Creek (H 4)	0.385	0.006	1.8 ± 0.5
	Ambapur Nagla (H 5/6)	0.393	0.014	2.4 ± 0.7
	Kernouve (H 6)	0.443	0.060	5.8 ± 1.6
	Ausson (L 5)	0.425	0.043	6.2 ± 1.7
	Peetz (L 6)	0.399	0.019	2.8 ± 0.8

[a] Calculated with assumed fission ratio of $(^{134}Xe/^{132}Xe)_f = 1.45 \pm 0.39$ which includes fission compositions from neutron induced fission and ^{244}Pu natural fission (see text). Errors are from uncertainties in this assumed ratio.

Table 12.

Temp. (°C)	% Blank	% Spallation	% Fission	$(^{128}Xe/^{132}Xe)_{cor}$	$(^{129}Xe/^{132}Xe)_{cor}$
			Bjurböle for Menow		
1100	0.6 ± 0.2	0.0 ± 0.1	14.1 ± 5.2	3.7097 ± 0.2322	1.9783 ± 0.1243
1200	0.1 ± 0.0	0.0 ± 0.0	2.8 ± 1.4	2.3282 ± 0.0336	1.8727 ± 0.0280
1300	0.1 ± 0.0	0.0 ± 0.0	3.1 ± 1.5	2.6827 ± 0.0414	2.0067 ± 0.0311
1400	0.1 ± 0.0	0.0 ± 0.0	0.8 ± 0.9	1.1332 ± 0.0113	1.4167 ± 0.0148
1500	0.1 ± 0.0	0.0 ± 0.0	2.5 ± 1.3	1.6119 ± 0.0228	1.6156 ± 0.0230
1600	1.4 ± 0.6	0.0 ± 0.0	6.0 ± 2.5	2.1140 ± 0.0880	1.7040 ± 0.0821
1650	2.3 ± 0.9	0.1 ± 0.1	3.2 ± 1.8	2.2725 ± 0.1726	1.8829 ± 0.1044
			Menow (H 4)		
1100	0.0 ± 0.0	0.0 ± 0.0	2.3 ± 1.2	0.1227 ± 0.0017	0.9948 ± 0.0130
1100(2)	0.2 ± 0.1	0.0 ± 0.0	2.6 ± 1.4	0.1979 ± 0.0040	1.0069 ± 0.0166
1200	0.1 ± 0.0	0.0 ± 0.0	3.8 ± 1.7	0.3020 ± 0.0058	1.0799 ± 0.0192
1300	0.1 ± 0.0	0.0 ± 0.1	8.0 ± 3.1	0.7605 ± 0.0257	1.3372 ± 0.0452
1400	0.1 ± 0.0	0.2 ± 0.1	6.3 ± 2.5	0.9010 ± 0.0244	1.4212 ± 0.0386
1500	0.1 ± 0.0	0.0 ± 0.1	4.3 ± 1.8	0.9242 ± 0.0175	1.3904 ± 0.0264
1600	0.5 ± 0.2	0.0 ± 0.1	6.0 ± 3.4	0.9655 ± 0.0374	1.4430 ± 0.0574
1650	1.4 ± 0.6	0.0 ± 0.0	5.7 ± 2.4	1.0600 ± 0.0417	1.5442 ± 0.0673

Table 13.

Temp. (°C)	% Blank	% Spallation	% Fission	$(^{128}Xe/^{132}Xe)_{cor}$	$(^{129}Xe/^{132}Xe)_{cor}$
			Bjurböle for Nadiabondi		
1100	0.1 ± 0.1	0.0 ± 0.1	5.0 ± 2.1	2.6712 ± 0.0603	1.8219 ± 0.0423
1200	0.0 ± 0.0	0.0 ± 0.0	2.6 ± 1.3	3.1296 ± 0.0422	2.1920 ± 0.0301
1300	0.0 ± 0.0	0.0 ± 0.0	2.0 ± 1.2	2.0450 ± 0.0251	1.7539 ± 0.0218
1400	0.0 ± 0.0	0.0 ± 0.0	2.4 ± 1.2	1.0357 ± 0.0135	1.4088 ± 0.0182
1500	0.1 ± 0.0	0.0 ± 0.1	4.5 ± 1.9	2.2174 ± 0.0454	1.9416 ± 0.0389
1600	0.5 ± 0.3	0.3 ± 0.1	6.3 ± 2.5	2.7719 ± 0.0964	2.0005 ± 0.0801
1650	0.7 ± 0.4	0.0 ± 0.0	5.0 ± 2.1	1.4655 ± 0.0426	1.2546 ± 0.0395
			Nadiabondi (H 5)		
1100	0.1 ± 0.1	0.2 ± 0.1	0.2 ± 0.9	1.1144 ± 0.0128	1.3212 ± 0.0153
1200	0.0 ± 0.0	0.1 ± 0.1	0.6 ± 0.9	0.5986 ± 0.0062	1.2308 ± 0.0123
1300	0.0 ± 0.0	0.1 ± 0.1	0.8 ± 0.9	0.5689 ± 0.0060	1.2341 ± 0.0121
1400	0.0 ± 0.0	0.1 ± 0.1	0.9 ± 1.0	0.4990 ± 0.0054	1.1944 ± 0.0124
1500	0.0 ± 0.0	0.0 ± 0.0	2.6 ± 1.3	0.4404 ± 0.0060	1.1652 ± 0.0160
1600	0.5 ± 0.3	0.0 ± 0.0	3.5 ± 1.7	0.8880 ± 0.0568	1.4772 ± 0.0391
1650	0.5 ± 0.3	0.4 ± 0.1	3.1 ± 2.5	0.6187 ± 0.0409	1.2891 ± 0.0480

Table 14.

Temp. (°C)	% Blank	% Spallaiton	% Fission	$(^{128}Xe/^{132}Xe)_{cor}$	$(^{129}Xe/^{132}Xe)_{cor}$
			Bjurböle for Beaver Creek		
1100	0.3 ± 0.2	0.0 ± 0.0	5.2 ± 2.2	0.8882 ± 0.0229	1.5756 ± 0.0449
1200	0.0 ± 0.0	0.0 ± 0.0	1.1 ± 1.0	0.8553 ± 0.0092	1.8959 ± 0.0208
1300	0.0 ± 0.0	0.0 ± 0.0	1.2 ± 1.0	0.9846 ± 0.0102	2.0341 ± 0.0209
1350	0.0 ± 0.0	0.0 ± 0.0	1.1 ± 1.0	0.5874 ± 0.0067	1.6228 ± 0.0168
1400	0.0 ± 0.0	0.0 ± 0.0	0.6 ± 0.9	0.4186 ± 0.0041	1.4371 ± 0.0145
1450	0.0 ± 0.0	0.0 ± 0.0	1.2 ± 1.0	0.4331 ± 0.0054	1.4504 ± 0.0154
1500	0.0 ± 0.0	0.0 ± 0.0	2.0 ± 1.2	0.6604 ± 0.0100	1.7344 ± 0.0227
1600	0.2 ± 0.2	1.9 ± 0.7	9.0 ± 3.7	1.0381 ± 0.0535	2.2326 ± 0.1351
1650	1.6 ± 1.2	0.0 ± 0.0	0.0 ± 0.0	0.9192 ± 0.0424	2.0153 ± 0.0975
			Beaver Creek (H 4)		
1100	0.6 ± 0.3	0.0 ± 0.0	3.7 ± 5.0	1.0214 ± 0.1095	1.3430 ± 0.1374
1200	0.1 ± 0.1	0.1 ± 0.1	0.1 ± 1.6	0.6166 ± 0.0225	1.7188 ± 0.0508
1300	0.0 ± 0.0	0.0 ± 0.0	1.1 ± 1.1	0.4266 ± 0.0068	1.5278 ± 0.0196
1350	0.0 ± 0.0	0.0 ± 0.0	0.4 ± 1.0	0.4107 ± 0.0065	1.4786 ± 0.0194
1400	0.0 ± 0.0	0.0 ± 0.0	0.8 ± 1.2	0.3444 ± 0.0094	1.4132 ± 0.0218
1450	0.0 ± 0.0	0.0 ± 0.0	0.0 ± 0.0	0.3788 ± 0.0082	1.4220 ± 0.0157
1550	0.0 ± 0.0	0.4 ± 0.1	1.0 ± 1.2	0.5204 ± 0.0112	1.6162 ± 0.0314
1600	0.1 ± 0.0	0.0 ± 0.0	0.8 ± 1.3	0.7285 ± 0.0161	1.8046 ± 0.0307
1650	0.3 ± 0.1	0.0 ± 0.0	1.6 ± 3.8	0.7054 ± 0.0568	1.8466 ± 0.1055

Table 15.

Temp. (°C)	% Blank	% Spallation	% Fission	$(^{128}Xe/^{132}Xe)_{cor}$	$(^{129}Xe/^{132}Xe)_{cor}$
			Bjurböle for Ambapur Nagly		
1100	0.0 ± 0.0	0.0 ± 0.0	1.5 ± 1.1	1.0625 ± 0.0116	2.1320 ± 0.0232
1200	0.0 ± 0.0	0.0 ± 0.0	1.1 ± 1.0	0.6278 ± 0.0063	1.6488 ± 0.0164
1300	0.0 ± 0.0	0.0 ± 0.0	0.9 ± 0.9	0.4672 ± 0.0049	1.4923 ± 0.0147
1350	0.1 ± 0.1	0.0 ± 0.0	0.4 ± 1.0	0.8230 ± 0.0098	1.8627 ± 0.0267
1400	0.2 ± 0.1	0.0 ± 0.0	0.7 ± 1.2	0.9719 ± 0.0157	2.0662 ± 0.0389
1450	0.1 ± 0.1	0.0 ± 0.0	1.4 ± 1.1	1.0480 ± 0.0121	2.1605 ± 0.0296
1500	0.2 ± 0.1	0.0 ± 0.0	0.6 ± 1.1	1.0006 ± 0.0149	2.1051 ± 0.0407
1600	2.1 ± 1.4	5.4 ± 1.3	5.2 ± 2.6	0.9509 ± 0.0705	2.2342 ± 0.2343
1650	4.0 ± 2.8	11.5 ± 4.9	6.9 ± 4.3	0.0780 ± 0.1067	1.3630 ± 0.2928
			Ambapur Nagla (H 5/6)		
1100	0.5 ± 0.1	0.0 ± 0.0	4.5 ± 1.9	0.4782 ± 0.0102	1.4427 ± 0.0317
1200	0.3 ± 0.1	0.0 ± 0.0	2.0 ± 1.2	0.4103 ± 0.0054	1.4184 ± 0.0193
1300	0.2 ± 0.0	0.0 ± 0.0	1.6 ± 1.1	0.3882 ± 0.0048	1.3774 ± 0.0170
1350	0.4 ± 0.1	0.0 ± 0.0	1.2 ± 1.0	0.5331 ± 0.0066	1.5092 ± 0.0213
1400	2.3 ± 0.5	0.0 ± 0.0	2.1 ± 1.3	0.6361 ± 0.0140	1.6000 ± 0.0514
1450	3.0 ± 0.7	0.0 ± 0.0	3.0 ± 1.7	0.6728 ± 0.0167	1.6984 ± 0.0646
1500	0.6 ± 0.1	0.0 ± 0.0	1.1 ± 1.2	0.6939 ± 0.0135	1.6711 ± 0.0272
1600	1.8 ± 0.4	0.0 ± 0.0	3.3 ± 1.7	0.6783 ± 0.0155	1.6627 ± 0.0467
1650	21.8 ± 7.6	0.0 ± 0.0	0.0 ± 0.0	0.3525 ± 0.1329	0.9977 ± 0.5314

0.381) which is within the errors identical to AVCC would not change matters to a significant degree. Atmosphere appears to be the least likely trapped component although its contribution cannot be ignored especially above 1500 °C where the blank contribution is expected to be somewhat higher. Noteworthy is that most of the high temperature fractions do not define a straight line, but fall in a field defined by the trapped value and extremes in fission composition. The 1400 °C and, to a less extent, the 1650 °C fractions lie above the field defined by the various compositions implying a trapped component with a higher $^{130}Xe/^{132}Xe$ ratio, but since the existence of such a trapped value cannot be determined from the technique we have treated these fractions as mixtures of the various known components. In order to correct ^{132}Xe (the reference isotope used in the I-^{129}Xe

Table 16.

Temp. (°C)	% Blank	% Spallation	% Fission	$(^{128}Xe/^{132}Xe)_{cor}$	$(^{129}Xe/^{132}Xe)_{cor}$
			Bjurböle for Kernouve		
1100	1.2 ± 0.0	0.0 ± 0.0	2.9 ± 1.4	1.2471 ± 0.0214	1.7213 ± 0.0307
1200	0.1 ± 0.0	0.0 ± 0.0	1.8 ± 1.1	0.9940 ± 0.0115	2.0762 ± 0.0240
1300	0.1 ± 0.0	0.0 ± 0.0	1.5 ± 1.0	0.6268 ± 0.0066	1.6748 ± 0.0180
1350	0.1 ± 0.0	0.0 ± 0.0	1.2 ± 1.0	0.4418 ± 0.0049	1.4780 ± 0.0160
1400	0.2 ± 0.0	0.0 ± 0.0	1.8 ± 1.1	0.4896 ± 0.0059	1.5639 ± 0.0187
1450	0.4 ± 0.0	0.0 ± 0.0	2.0 ± 1.2	0.6886 ± 0.0098	1.8086 ± 0.0256
1500	0.9 ± 0.0	0.0 ± 0.1	0.4 ± 1.2	0.8103 ± 0.0262	1.9281 ± 0.0378
1600	3.6 ± 0.1	0.0 ± 0.0	0.4 ± 1.3	0.7504 ± 0.0164	1.8163 ± 0.0398
1650	1.6 ± 0.1	0.0 ± 0.0	2.1 ± 1.3	0.9520 ± 0.0155	2.1647 ± 0.0339
			Kernouve (H 6)		
1300	2.8 ± 0.1	0.0 ± 0.0	8.2 ± 3.1	0.2695 ± 0.0100	1.3919 ± 0.0497
1350	1.4 ± 0.0	0.0 ± 0.0	3.0 ± 1.4	0.1938 ± 0.0037	1.2629 ± 0.0205
1400	2.4 ± 0.1	0.0 ± 0.0	1.2 ± 1.0	0.1439 ± 0.0029	1.1870 ± 0.0169
1450	1.4 ± 0.0	0.1 ± 0.1	1.5 ± 1.1	0.1791 ± 0.0041	1.2619 ± 0.0171
1500	1.6 ± 0.0	0.0 ± 0.1	0.7 ± 1.0	0.1872 ± 0.0041	1.2687 ± 0.0198
1600	2.7 ± 0.1	0.0 ± 0.0	0.0 ± 0.0	0.2583 ± 0.0038	1.4099 ± 0.0265
1650	11.4 ± 0.3	0.0 ± 0.0	2.2 ± 4.3	0.2020 ± 0.0195	1.4690 ± 0.1501

Table 17.

Temp.(°C)	% Blank	% Spallation	% Fission	$(^{128}Xe/^{132}Xe)_{cor}$	$(^{129}Xe/^{132}Xe)_{cor}$
			Bjurböle for Ausson		
1100	0.0 ± 0.0	0.0 ± 0.0	0.4 ± 1.0	0.7867 ± 0.0083	1.8372 ± 0.0211
1200	0.0 ± 0.0	0.0 ± 0.0	0.9 ± 1.0	1.0112 ± 0.0100	2.1766 ± 0.0220
1300	0.0 ± 0.0	0.0 ± 0.0	0.8 ± 0.9	0.4890 ± 0.0051	1.5515 ± 0.0152
1350	0.0 ± 0.0	0.0 ± 0.0	0.1 ± 0.9	0.3676 ± 0.0039	1.4131 ± 0.0139
1400	0.1 ± 0.0	0.0 ± 0.0	1.3 ± 1.0	0.5513 ± 0.0071	1.6919 ± 0.0203
1450	0.1 ± 0.1	0.0 ± 0.0	1.2 ± 1.1	0.8414 ± 0.0135	2.0157 ± 0.0309
1500	0.2 ± 0.1	0.0 ± 0.0	0.8 ± 1.2	1.0964 ± 0.0169	2.3057 ± 0.0402
1600	0.3 ± 0.2	0.0 ± 0.0	4.1 ± 1.9	1.1642 ± 0.0457	2.4269 ± 0.0893
1650	1.8 ± 1.2	0.0 ± 0.0	0.0 ± 0.0	0.6854 ± 0.0277	1.9223 ± 0.1522
			Ausson (L 5)		
1100	0.3 ± 0.1	0.6 ± 0.1	3.1 ± 1.5	0.3888 ± 0.0086	1.4467 ± 0.0291
1200	0.2 ± 0.1	0.4 ± 0.1	3.3 ± 1.6	0.4029 ± 0.0074	1.4940 ± 0.0276
1300	0.1 ± 0.0	0.1 ± 0.1	2.1 ± 1.2	0.3479 ± 0.0049	1.4217 ± 0.0194
1350	0.1 ± 0.0	0.0 ± 0.1	1.4 ± 1.1	0.5371 ± 0.0068	1.6720 ± 0.0191
1400	0.4 ± 0.2	0.0 ± 0.0	0.9 ± 1.1	0.5424 ± 0.0098	1.7216 ± 0.0325
1450	0.8 ± 0.3	0.0 ± 0.0	2.7 ± 1.6	0.4953 ± 0.0153	1.7580 ± 0.0412
1500	2.4 ± 0.9	0.0 ± 0.0	1.6 ± 1.3	0.4201 ± 0.0257	1.5698 ± 0.0801
1600	0.7 ± 0.3	0.0 ± 0.0	0.5 ± 1.2	0.4388 ± 0.0163	1.5368 ± 0.0362
1650	10.0 ± 5.8	0.0 ± 0.0	13.3 ± 6.5	0.3901 ± 0.0823	1.6082 ± 0.4263

correlation diagram) for fission of any type, our approach has been simply to make this correction by partitioning the $^{134}Xe/^{132}Xe$ ratio between a range of trapped values $^{134}Xe/^{132}Xe = 0.3785 \pm 0.0095$ including BEOC 12 and atmospheric [22], and a range of fission values, $^{134}Xe/^{132}Xe = 1.45 \pm 0.39$ including spontaneous fission from ^{244}Pu and neutron-induced fission from ^{235}U. Using these assumptions, we have tabulated $^{132}Xe_f/^{132}Xe_{total}$ and the $[^{132}Xe_f]$ concentration in Table 11. The percentage fission appearing in the high temperature fractions at ^{132}Xe as well as the final corrected $(^{128}Xe/^{132}Xe)_{cor}$ and $(^{129}Xe/^{132}Xe)_{cor}$ ratios are summarized in Tables 12–18. While these corrections are not negligible, they are still generally rather small in the important high temperature fractions and by no means dominant.

Table 18.

Temp. (°C)	% Blank	% Spallation	% Fission	$(^{128}Xe/^{132}Xe)_{cor}$	$(^{129}Xe/^{132}Xe)_{cor}$
			Bjurböle for Peetz		
1100	0.9 ± 0.1	0.0 ± 0.0	2.2 ± 1.2	1.1102 ± 0.0147	1.9371 ± 0.0270
1200	0.3 ± 0.0	0.0 ± 0.0	1.0 ± 1.0	0.8360 ± 0.0089	2.0119 ± 0.0218
1250	0.5 ± 0.0	0.0 ± 0.0	0.9 ± 1.0	0.7789 ± 0.0084	1.8974 ± 0.0202
1300	0.6 ± 0.0	0.0 ± 0.0	1.4 ± 1.0	0.3997 ± 0.0047	1.4712 ± 0.0167
1350	0.6 ± 0.0	0.0 ± 0.0	1.4 ± 1.0	0.3997 ± 0.0047	1.4712 ± 0.0167
1400	0.7 ± 0.0	0.0 ± 0.0	0.8 ± 1.0	0.3897 ± 0.0044	1.4533 ± 0.0173
1500	0.8 ± 0.1	0.0 ± 0.0	2.4 ± 1.3	0.6773 ± 0.0091	1.8712 ± 0.0267
1600	4.2 ± 0.3	0.0 ± 0.0	2.9 ± 1.6	0.9159 ± 0.0180	2.2253 ± 0.0640
1650	18.0 ± 1.8	0.0 ± 0.0	11.2 ± 5.2	1.1647 ± 0.0960	2.7384 ± 0.3203
			Peetz (L 6)		
1100	0.7 ± 0.1	1.6 ± 0.3	15.2 ± 5.7	2.9294 ± 0.2114	1.3445 ± 0.0963
1200	0.5 ± 0.1	1.0 ± 0.2	15.7 ± 5.8	0.6364 ± 0.0447	1.2378 ± 0.0888
1250	0.4 ± 0.1	0.3 ± 0.1	5.8 ± 2.3	0.2334 ± 0.0067	1.2197 ± 0.0341
1300	0.2 ± 0.0	0.1 ± 0.1	1.6 ± 1.1	0.1581 ± 0.0026	1.1343 ± 0.0138
1350	0.1 ± 0.0	0.0 ± 0.0	0.5 ± 0.9	0.1348 ± 0.0021	1.1068 ± 0.0124
1400	0.1 ± 0.0	0.1 ± 0.1	0.8 ± 1.0	0.1463 ± 0.0030	1.1504 ± 0.0144
1500	0.1 ± 0.0	0.0 ± 0.0	0.0 ± 0.9	0.1958 ± 0.0031	1.2148 ± 0.0187
1600	0.6 ± 0.1	0.0 ± 0.0	0.0 ± 0.0	0.1828 ± 0.0045	1.1921 ± 0.0266
1650	8.3 ± 1.8	0.0 ± 0.0	0.0 ± 0.0	0.1216 ± 0.0699	1.0726 ± 0.3668

d) I and Te Contents

After blank, spallation, and fission corrections ^{128}Xe and ^{131}Xe are mixtures of trapped gas and neutron produced isotopes from $^{127}I(n, \gamma\beta^-)^{128}Xe$ and from both $^{130}Te(n, \gamma\beta^-, \beta^-)^{131}Xe$ and $^{130}Ba(n, \gamma\beta^+, \beta^+)^{131}Xe$. Using the Bjurböle standard as a flux monitor by assuming the slopes of the Bjurböle correlation lines correspond to $(^{129}I/^{127}I)_0 = 1.09 \times 10^{-4}$ we may calculate I and Te abundances from the total ^{128}Xe and ^{131}Xe excesses remaining after subtraction of trapped, spallation, and fission components. The I-contents may be determined from the $^{128}Xe^*/^{127}I$ ratio which is directly obtained from the slope of the high temperature correlation line and the $(^{129}I/^{127}I)_0$ for Bjurböle. For Te, we need the absolute neutron capture cross section $\sigma(^{130}Te)$ and, in addition $\sigma(^{127}I)$ to determine the fluence. They were taken as 0.27 barns and 6.4 barns, respectively. The tabulated I and Te abundances which should be regarded as lower limits because of possible gas loss, are listed in Table 19. We did not consider ^{131}Xe production from ^{130}Ba justified by the assumption that Ba and Te occur in approximately their cosmic abundance ratio [23] in which case the ^{131}Xe production from Te overwhelmingly dominates. There is some indication from the data that the L-group is somewhat more Te rich than the H-group, but the difference is not impressive enough, in light of the methods limitations, to warrant a firm conclusion. No trends in the I abundances among the petrological classes or differences between chemical groups are observable. The only striking feature is that the Bjurböle (L 4) standard has 3—5 times higher I-content than the other meteorites, but it appears to have nothing to do with the fact that it is an L-chondrite or has a metamorphic grade of 4. Considering the limitations of the technique, the Bjurböle I contents we have determined (24 ppb) compare well with that (32 ppb) from Drozd and Podosek [7].

e) The I-Xe Correlation

After all of the above mentioned corrections, the system of $(^{128}Xe/^{132}Xe)_{cor}$ and $(^{129}Xe/^{132}Xe)_{cor}$ consists of only trapped gas and the I-related components, in particular $^{128}Xe^*$ and $^{129}Xe^*$ (correlated I-xenon). The conventional I-Xe correlation diagram is made by plotting $(^{129}Xe/^{132}Xe)_{cor}$ vs. $(^{128}Xe/^{132}Xe)_{cor}$ for each temperature fraction. A correlation occurs when ^{129}Xe and ^{128}Xe are released in constant proportions and a straight line is defined by the temperature fractions, which is assumed to connect the two components: the trapped component $(^{129}Xe/^{132}Xe)_t$ which is determined by the assumption of a $(^{128}Xe/^{132}Xe)_t$ ratio and an I-component which plots at infinity because no ^{132}Xe is present. The slope of the correlation

line ($^{129}Xe^*/^{128}Xe^*$) may by translated into an initial iodine ratio $(^{129}I/^{127}I)_0$ from the $^{128}Xe^*/^{127}I$ production ratio (measured in this case by the Bjurböle standard) and is interpreted to represent the iodine ratio present in the mineral phases defining the correlation line at the time when xenon was retained. Formation ages with respect to Bjurböle (assuming $(^{129}I/^{127}I)_0 = 1.09 \times 10^{-4}$ for Bjurböle) may be simply determined from

$$\Delta t = \tau \ln (m_{Bju}/m_{Met} f)$$

where $\tau = 25$ m.y., $m_{Bju} = (^{129}Xe^*/^{128}Xe^*)$ for Bjurböle, $m_{Met} = (^{129}Xe^*/^{128}Xe^*)$ for the meteorite and $f = \Phi_{Met}/\Phi_{Bju}$, the relative flux factor from Table 1. More precisely, the "formation ages" refer to the Xe-retention age in the high temperature I-phases of the respective meteorites. In Fig. 4 — 10 are presented the conventional I-Xe correlation diagrams for the individual meteorites and their respective Bjurböle standard. Lower temperature fractions which did not correlate are below and to the right of the correlation line. In cases where the last uncorrelated lower temperature fraction was not too far to the right, these were plotted as open circles. The ages relative to Bjurböle, initial $(^{129}I/^{127}I)_0$ ratios, and $(^{129}Xe/^{132}Xe)_t$ ratios are summarized in Table 19 and Figure 12.

Correlation lines were determined by a York [24] fitting program which includes errors in the data points. The quality of the fit depends not only on how near the data points plot along the correlation line, but also on the amount of total variation in the ratios as well. In a study which is primarily aimed at obtaining information in bulk meteorites as opposed to mineral and inclusion separates one is faced with the problem of the dominance of the trapped gas component. Therefore, the total variability in the $^{129}Xe/^{132}Xe$ is somewhat limited; the typical range covering 160% of the trapped value. The Bjurböle standard has the widest range of variability of 250%, and Peetz has the narrowest range of 118%. This may be compared to mineral and inclusion separates such as the Orgueil (C 1) and Murchison (C 2) magnetites [6], silicates from I AB iron meteorites [25], and inclusions from Allende [26, 27] in which enhancements of 3—25 fold over the lowest measured ($^{129}Xe/^{132}Xe$) ratio are observed. Most recently, an infinite $^{129}Xe/^{132}Xe$ ratio has been discovered in a halogen-rich inclusion from Allende [28]. The dominance of the trapped component in the meteorites of this study consequently causes the slope errors to be more

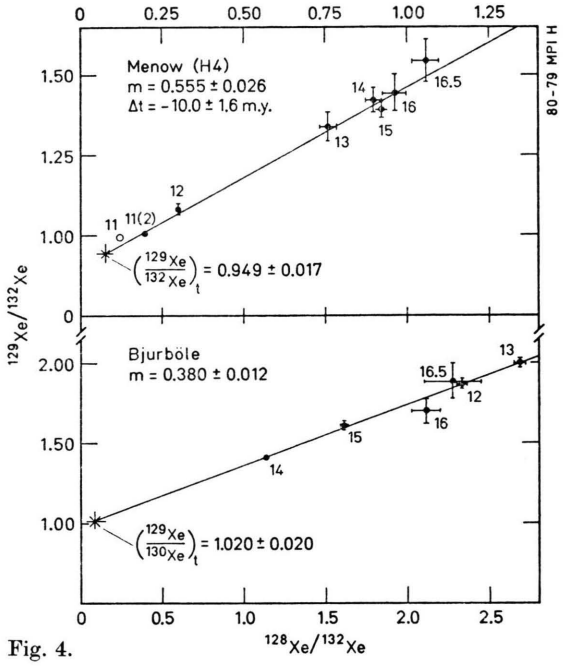

Fig. 4.

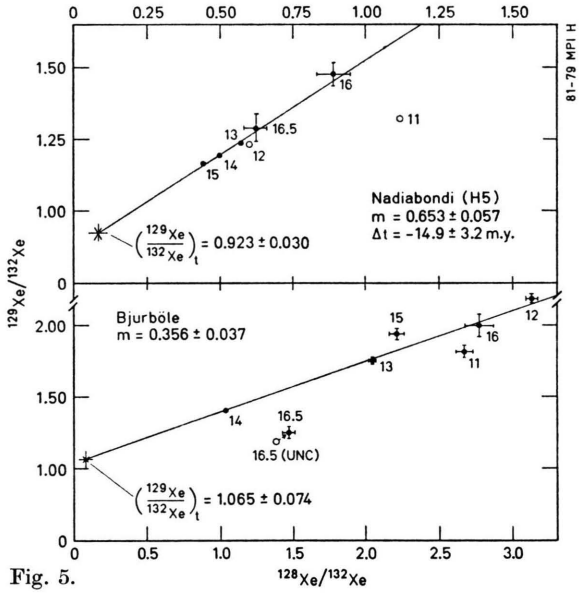

Fig. 5.

Figs. 4 and 5. I-Xe correlation diagrams for the H-chondrites Menow (H 4) and Nadiabondi (H 5) and their respective Bjurböle standards which were n-irradiated in the K-1 irradiation. The slopes $m = (^{129}Xe^*/^{128}Xe^*)$ were determined from a York [24] last squares fit, and the trapped ratio $(^{129}Xe/^{132}Xe)_t$ was determined where $(^{128}Xe/^{132}Xe)_t$ was assumed to be 0.082 [15]. The uncorrected (UNC) value of the 1650° fraction (open circle) of the Bjurböle standard for Nadiabondi indicates that it was probably undercorrected and was, therefore, ignored in the least squares fit (see text). The last lower temperature fractions which did not correlate, but were near enough to the correlation line to be seen in the diagram, are also plotted as open circles.

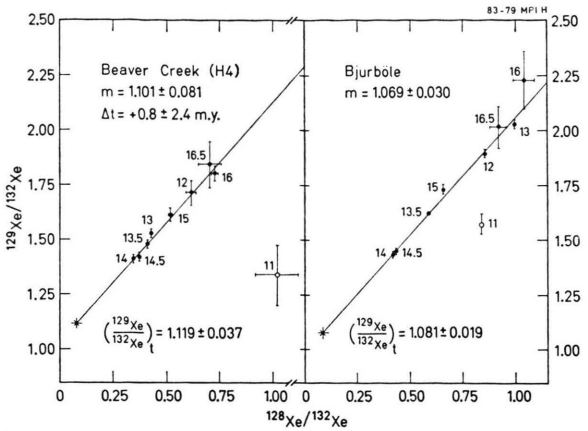

Fig. 6.

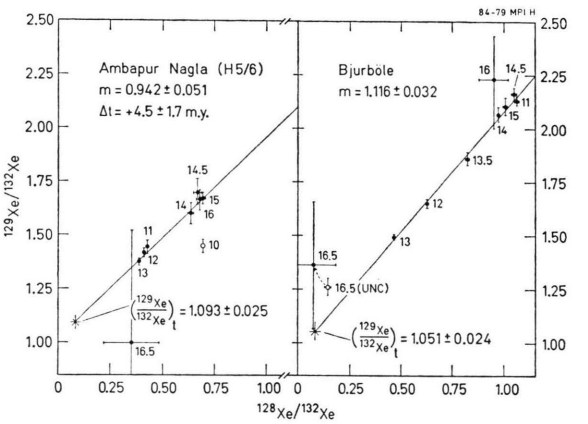

Fig. 7.

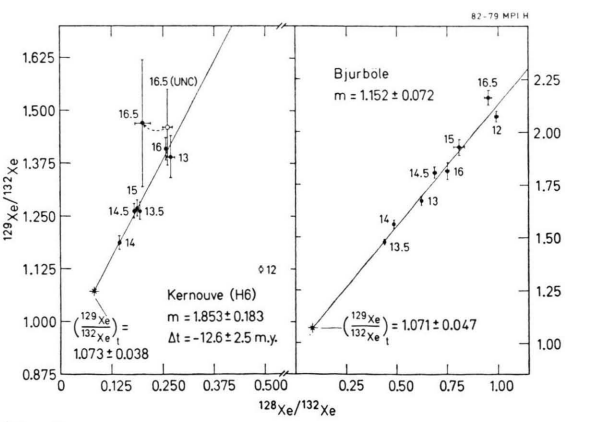

Fig. 8.

Figs. 6, 7 and 8. I-Xe correlation diagrams for the H-chondrites Beaver Creek (H 4), Ambapur Nagla (H 5/6), Kernouve (H 6), and their respective Bjurböle standards which were irradiated in the K-2 irradiation.

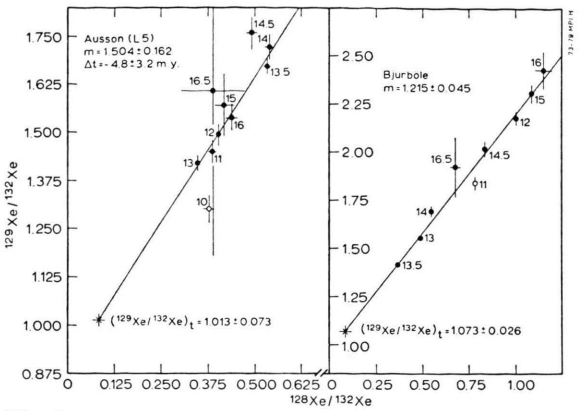

Fig. 9.

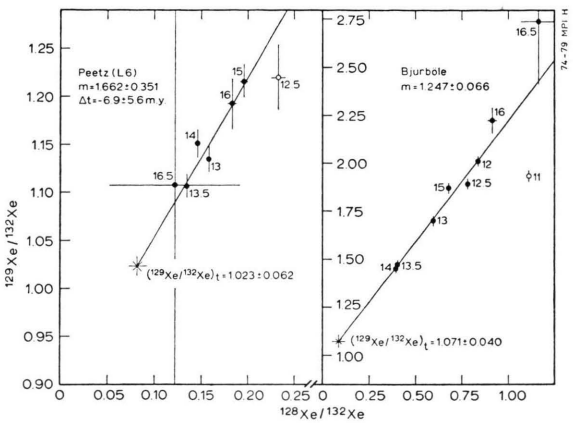

Fig. 10.

Figs. 9 and 10. I-Xe correlation diagrams for the L-chondrites Ausson (L 5), Peetz (L 6), and their respective Bjurböle standards which were irradiated in the K-2 irradiation.

sensitive to the various kinds of corrections than in the case of these separates and may lead to unattractively large age errors, like in the (worst) case of Peetz (L 6) ($\Delta t = -6.9 \pm 5.6$ m.y.). Furthermore, all correlations of this study begin, as is typical of ordinary chondrites, at high temperatures; the lowest correlated temperature fraction being 1100 °C (for a few Bjurböle standards). Recently, lower temperature fractions, beginning at 600 °C, have been observed to correlate in the Mundrabilla silicates [25] and inclusions from Allende (800 °C to 1050 °C) defining a correlation line distinct from that formed by the higher temperature fractions [26, 27]. We share the common belief that the uncorrelated lower temperature fractions observed in ordinary

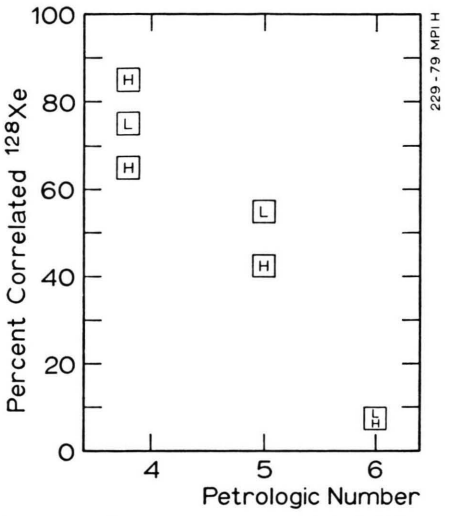

Fig. 11. The percentage correlated ^{128}Xe measuring the percentage I with which the ^{129}Xe excess is correlated vs. petrologic number for the chondrites of this study. Ambapur Nagla (H 5/6) was omitted based on uncertainty as to its classification (5 or 6 [9]). With 50% correlated ^{128}Xe it appears, from the xenon data, to more closely resemble petrologic type 5. The anticorrelation indicates that metamorphism has played a role in determining the extent to which the I-Xe record in these meteorites was preserved.

chondrites represent either preferential $^{129}Xe^*$ loss from less retentive sites or slow cooling of the meteorite parent body. This is supported by a correlation between petrologic grade and percentage of uncorrelated ^{128}Xe (see the complementary figures for the percentages of correlated ^{128}Xe in Table 19 and Figure 11).

H-Chondrites

The H-chondrites fail to show a correlation of petrologic number with age, and have large age variations within a single petrologic grade (cf. Menow (H 4), $\Delta t = -10$ m.y. and Beaver Creek (H 4), $\Delta t = +0.8$ m.y.). Moreover, three from the five H-chondrites, even within the positive extremes of the errors, are older than the Orgueil (C 1) and Murchison (C 2) magnetites (see Fig. 12) which were once believed to be dating the condensation phase of the solar nebula [5, 6]. They add to the Arapahoe (L 5) observation [7], the first ordinary chondrite found which predates these magnetites ($\Delta t = 9.9 \pm 0.8$ m.y.), and the Mundrabilla troilite ($\Delta t = -10.8 \pm 0.7$ m.y.), [24].

The Menow run was interrupted at 900 °C by the development of a hole in the quartz jacket of the furnace. The sample had to be removed to make the necessary repairs and was consequently contaminated by adsorbed air as well as by the presence of quartz fragments. A rerun was begun at 800 °C to drive off the atmospheric component dominant until the 1100 °C fraction, which was run twice to insure that this component was essentially removed. Some contamination must, however, be expected for the higher temperature fractions. An older age due to this contamination could only result if the real trapped $(^{129}Xe/^{132}Xe)_t$ value is greater than the atmospheric ratio, 0.983 and a dominant atmospheric release occurs at the higher temperatures (see Figure 4). Since the trapped ratio determined by the method is less (0.949 ± 0.017) than the atmospheric ratio such a possibility is ruled out. Thus, the Δt for Menow is most probably older than or equal to the -10 m.y. determined from this run. The other meteorites were run with no experimental problems and this includes Nadiabondi (H 5) and Kernouve (H 6) which are both older than Menow by -4.9 ± 3.6 m.y. and -2.6 ± 3.2 m.y., respectively.

L-Chondrites

Peetz (L 6) is characterized by the most dominant trapped component (see Figure 10). This is observed in the high temperature fractions of the spallation diagram (Fig. 2) as well. This large trapped component is corroborated in the Peetz phosphates [12] which are ten times more gas-rich than the bulk meteorite and 90 percent of the ^{132}Xe is trapped gas. The phosphates cannot, however, be the primary source of the trapped gas at the higher temperatures because of their very low abundance ($\sim 10^{-4}$ g phosphate/g bulk). They are also not the carriers of the high temperature I-Xe correlation in Peetz as no ^{129}Xe excesses were observed [12].

Both the L-chondrites, Ausson (L 5) and Peetz (L 6) have ages, Δt, that are older than Bjurböle (L 4) even within the errors which are quite large, -4.8 ± 3.2 m.y. and -6.9 ± 5.6 m.y., respectively. Within these errors they could be also older than the Orgueil (C 1) and Murchison (C 2) magnetite separates [6]. That meteorites with petrologic numbers 5 and 6 are older than one with petrologic number 4 contradicts a sequence of younger ages in the direction of increasing metamorphism, expected in a scenario in which meteorites formed in an environment with a homogeneous $^{129}I/^{127}I$

Table 19. Summary of results.

Irr.	Meteorite	$[^{132}Xe_t]$ $\times 10^{-10}$ cm^3 STP/g)	Δt (m.y.)	$(^{129}I/^{127}I)_0$ [a] $\times 10^{-4}$	$(^{129}Xe/^{132}Xe)_{total}$ [b]	$(^{129}Xe/^{132}Xe)_{trapped}$ [c]	[I] (ppb)	[Te] (ppm)	% corr. ^{128}Xe
K-1	Menow (H 4)	(2.5) [d]	-10.0 ± 1.6	1.63	(1.565 ± 0.004) [d]	0.949 ± 0.017	5	0.3	(64) [d]
	Nadiabondi (H.5)	3.4	-14.9 ± 3.2	1.98	1.223 ± 0.001	0.923 ± 0.030	5	0.3	42
	Beaver Creek (H 4)	3.0	$+ 0.8 \pm 2.4$	1.06	1.536 ± 0.004	1.119 ± 0.037	7	0.4	85
	Ambapur Nagla (H 5/6)	1.8	$+ 4.5 \pm 1.7$	0.91	1.414 ± 0.003	1.093 ± 0.025	6	0.4	50
	Kernouve (H 6)	0.9	-12.6 ± 2.8	1.80	1.272 ± 0.003	1.073 ± 0.038	8	0.4	6
K-2	Ausson (L 5)	1.4	$- 4.8 \pm 3.2$	1.32	1.500 ± 0.003	1.013 ± 0.073	5	0.5	54
	Peetz (L 6)	1.4	$- 6.9 \pm 5.6$	1.44	1.165 ± 0.003	1.023 ± 0.062	6	0.5	8
	Bjurböle (L 4)	5.7 (5.4) [e]	0	$\equiv 1.09$	1.755 ± 0.008	1.062 ± 0.008	24	0.5	75
	average								

[a] Calculated with the assumption that the Bjurböle initial $(^{129}I/^{127}I)_0$ ratio was 1.09×10^{-4}.

[b] Ratios are corrected for fission and spallation. The error given for the average of the seven Bjurböle standards is the standard deviation of the mean. All other errors are measurement errors.

[c] Calculated with the assumption that $(^{128}Xe/^{132}Xe)_t = 0.082$ (Murray composition [15]).

[d] $[^{132}Xe_t]$ and $(^{128}Xe/^{132}Xe)_{total}$ determined from unirradiated sample. Percentage correlated ^{128}Xe calculated after removal of 0.3×10^{-12} cm^3 STP/g ^{128}Xe contamination from air (see text).

[e] Calculated omitting two standards (for Beaver Creek and Ausson) which contained 14—17% more $^{132}Xe_t$ than the next highest fraction. With the exception of one standard (for Kernouve) which was predegassed at 800° for two hours to eliminate apparent contaminants all other $^{132}Xe_t$ contents were within 5% of one another.

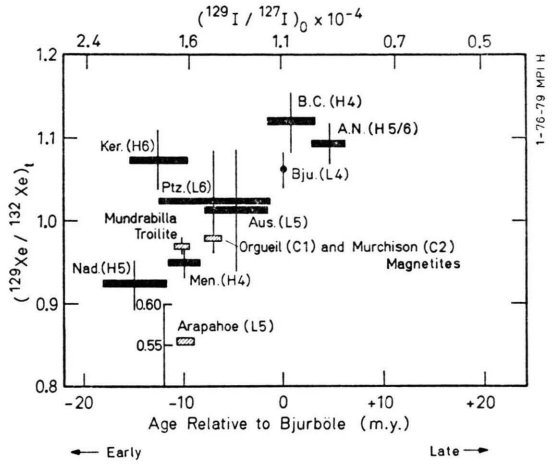

Fig. 12. Summary diagram of I-Xe results, including ages with respect to the Bjurböle standard, $(^{129}I/^{127}I)_0$ ratio at the time of xenon retention, based on the assumption that the Bjurböle initial $(^{129}I/^{127}I)_0$ ratio was 1.09×10^{-4}, and the trapped $(^{129}Xe/^{132}Xe)_t$ ratio determined from the I-Xe technique. The heavy dark lines indicate meteorites of this study; the Orgueil and Murchison magnetites are from Lewis and Anders [6], the Mundrabilla troilite is from Niemeyer [25], and Arapahoe is from Drozd and Podosek [7].

ratio, the observed differences in which reflect the time of Xe-retention which in turn would be dependent upon the metamorphic history of the meteorite parent body.

Discussion

a) Interpretation of the I-Xe Correlation

The classic interpretation of the I-Xe correlation is that the ^{129}Xe-^{128}Xe proportionality reflects *in situ* decay, preserved only in those retentive sites which were not disturbed by moderate metamorphism. This leads to the expectation that the percentage of I with which the ^{129}Xe is correlated (reflected by the percentage correlated ^{128}Xe), should be anticorrelated to the petrologic number, as we actually observe in Figure 11. However, there is an alternative model in which the initial state is one of no preserved correlation and the high temperature correlation is an artifact due to diffusion resulting from strong thermal stresses in the heating experiment. Huneke [29] has proposed that high temperature correlations which would be meaningless in terms of meteoritic origin could be produced in the laboratory by diffusive amalgamation of the parent (represented by the neutron produced gas atoms, e.g. ^{39}Ar, ^{128}Xe) and the daughter (e.g. ^{40}Ar, ^{129}Xe), at the lower temperatures. This would *require* that a significant portion of the lower temperature gas be uncorrelated. We dismiss this model on the following grounds: a) If the $^{129}Xe/^{128}Xe$ ratio is expected to approach a constant via diffusive amalgamation, then so should the $^{129}Xe/^{132}Xe$ ratio. This is in fact not observed, large variations in the $^{129}Xe/^{132}Xe$ ratio in the correlation diagram are often observed. b) Correlations occur even at low temperatures for some highly metamorphosed meteorites, such as the iron meteorite Mundrabilla, for which Niemeyer [25] has observed that 100% of the ^{129}Xe is correlated with the ^{128}Xe in removed silicate inclusions.

b) The Failure of the I-Xe Ages to Reflect Petrologic History

It is clear from the I-Xe analysis of the ordinary chondrites of this study that the role of shock and weathering effects could not alone be responsible for the lack of correlation between petrologic type and I-Xe age. It is also an obvious consequence of this result that metamorphic history was not the only factor (if at all) in assigning the initial $(^{129}I/^{127}I)$ ratio to the carriers of the high temperature I-Xe correlation in ordinary chondrites. This statement is of course highly dependent on the widely accepted assumption that all meteorites of a given class can be derived from a single parent body, and that the different classes formed at nearly the same time. If many bodies existed for a given class and the formation of them occurred at different times, then the lack of chronological order among the various chondrites could simply arise from the lack of synchronism in their individual metamorphic histories. Based on the observed anticorrelation between petrologic number and percent correlated ^{128}Xe, the metamorphic history does seem to have played a role in determining how much of the correlation survives. If one avoids appealing to the various imagined mechanisms in which the high temperature correlation is a consequence of or altered by I-Xe fractionation, then one is left with basically two avenues:

Homogeneous $(^{129}I/^{127}I)_0$ ratio for the solar nebula, ages are real, no metamorphic influence.

Here "no metamorphic influence" is intended to mean that no *ages* are influenced, although the lower temperature portions of the correlations may be

destroyed. This essentially defines the relative formation time to be the relative condensation time for the I-bearing phases in meteorites. This definition has always been applied to phases separated from carbonaceous condrites since they probably experienced little, if any, metamorphism; but implies, in this case, that the ordinary chondrites Arapahoe (L 5), Menow (H 4), Nadiabondi (H 5), and Kernouve (H 6) contain phases which began to condense some 8 m.y. prior to the Orgueil (C 1) and Murchison (C 2) magnetites (the age difference between the oldest meteorite, Nadiabondi, and the magnetite phases). Recently, Zaikowski [26, 27] has applied this interpretation to I-Xe ages of Allende inclusions for which two correlations for the same inclusion were observed; one at lower temperatures (800 °C—1050 °C) and another with a higher slope at temperatures greater than 1100 °C. Zaikowski [26, 27] assigned the lower temperature correlation to feldpathoids which he was able to identify and the higher temperature correlation to refractory minerals which were not identified and concluded from the slope differences that 3.7 m.y. elapsed between the condensation of the refractory minerals and the condensation of the low temperature feldspathoids. The refractory phases predate St. Severin (the standard used) by 18 m.y., corresponding to — 10 m.y. with respect to Bjurböle [2], or in the spirit of this interpretation about the same time the Menow and Arapahoe refractory phases condensed. More recently, Wasserburg and Huneke [28] have reported an I-Xe age very close to Bjurböle for a halogen-rich spherical chondrule from Allende containing sodalite, nepheline, olivine, and pyroxene. The largest and essentially pure $^{129}Xe^*$ release was observed between 900°—1100 °C near the melting temperature of pure sodalite, the phase which was suggested as the carrier of the I-Xe correlation. Thus, about 20 m.y. or more (the width of the I-Xe interval based primarily on high temperature correlations) could exist between condensations of refractory minerals and about 10 m.y. or more (the time difference between the ages for the feldspathoids) could exist between condensations of low temperature phases. The relative differences would require spatial variations in the initial solar nebula temperature although, in light of the limited data available for low temperature phases, spatial variations in the condensation rate alone could give indistinguishable results.

Inhomogeneous $(^{129}I/^{127}I)_0$ ratio for the solar nebula, ages meaningless, no metamorphic influence required, but possible.

In this case only the $(^{129}I/^{127}I)_0$ ratio extracted from the high temperature correlation is meaningful, and provides a measure of the degree to which the inhomogeneity existed. From meteorites for which I-Xe correlations exist, it appears that variations in the $(^{129}I/^{127}I)_0$ ratio of a factor of two or more could have existed.

There is no direct statement in this scenario of whether ^{129}I was alive or dead in the solar system. Clayton [30] has suggested that the inhomogenous $(^{129}I/^{127}I)_0$ ratio could be due to the presence of presolar grains in which the high temperature correlation survived but the ^{129}I was dead at the time of solar system formation. The fact, however, that the excess ^{129}Xe can be correlated with 85% (or even more) of the normal chondritic portion of the I forces the model to explain the existence of most of the normal I in this way, which is rather unlikely. This problem can only be circumvented if the I-Xe record is preserved in a single mineral phase which is identical for both the presolar condensates and the solar nebula condensates. The existence of two separate correlation lines for the high and low temperature phases of a single Allende inclusion [26, 27], as well as variable ^{129}Xe excesses observed in phosphates [12], which cannot account for all of the $^{129}Xe^*$ in the bulk meteorite suggests that the I does not sit in a single mineral phase. We therefore, on these grounds, dismiss the presolar grain origin of the I-Xe anomaly as a possible explanation for the lack of correlation of age with petrologic number and maintain that ^{129}I was alive at the time of solar system formation.

Although, in this picture, inhomogeneities in the initial $(^{129}I/^{127}I)_0$ ratio would exist within the solar nebula, metamorphism could have played a role in determining when the I-Xe clock was set within a single meteorite parent body. If it formed in a region characterized by a single $(^{129}I/^{127}I)_0$ ratio then the various petrologic types 1—6 derived from this parent body would be expected to follow the sequence of younger I-Xe ages in the direction of higher petrologic numbers. Comparison of two identical petrologic types derived from separate parent bodies forming in regions characterized by different $(^{129}I/^{127}I)_0$ ratios, could then result in "age differences" which would give rise to the lack

of order observed in Figure 12. Similar failure of such a sequence to occur would result if a single meteorite parent body was characterized by isotopic inhomogeneities in iodine.

c) Comment on the $(^{129}Xe/^{132}Xe)_t$ ratio

Podosek [2] had earlier recognized that not all meteorites can be characterized by a single $(^{129}Xe/^{132}Xe)_t$ trapped ratio resembling atmospheric value of 0.983 or a solar value of about 1, but substantial differences may exist. The most extreme values in this ratio observed to date are 0.56 (Arapahoe (L 5) [7]) and 3.50 (Landes I AB iron meteorite [25]). These values are, however, highly extreme; more typical values lie between 0.8 and 1.3 [2]. The data which we present in this work lie in the range between 0.92 and 1.12. The effect of uncertainties in the adopted $(^{128}Xe/^{132}Xe)_t$ ratio on the $(^{129}Xe/^{132}Xe)_t$ ratio is insignificant ($< 1\%$). It was also recognized that there exists a trend of increasing trapped $(^{129}Xe/^{132}Xe)_t$ values toward younger I-Xe ages [2]. We observe this trend as well in our data (see Figure 12). In any model which maintains that the ages are meaningful, this observation can be simply explained as the result of ^{129}I decay in which daughter product ^{129}Xe equilibrates with the trapped gas phase (either in Xe depleted regions of the solar nebula or an internal atmosphere) before the ^{129}I-^{129}Xe system was closed [2]. If I-Xe ages are disturbed due to inhomogeneities in the $(^{129}I/^{127}I)_0$ ratio, then the increase in the trapped $(^{129}Xe/^{132}Xe)_t$ ratio in the direction of lower $(^{129}I/^{127}I)_0$ ratios is decoupled to *some* degree from time. Thus, spatial inhomogeneities in the $(^{129}I/^{127}I)_0$ ratio should also be accompanied by spatial variations in the $(^{129}Xe/^{132}Xe)_t$ ratio, in such a way that high $(^{129}I/^{127}I)_0$ ratios are associated with low $(^{129}Xe/^{132}Xe)_t$ ratios.

Conclusions

The nature of ^{129}I as a chronometer for early solar system events remains an open question. If only condensation is being dated, then it apparently occurred at different places in the solar nebula over a time period of the order of 10^7 y. If early metamorphic events are, in addition, being dated, separation in time and location may be required for parent body formation, instead of (*or* because of) spatiotemporal variability for condensation, in order to explain the lack of correlation of petrologic type with I-Xe age. A shorter time scale could have, however, existed for the condensation-accretion process if the I-Xe ages are disturbed by isotopic inhomogeneities in the $(^{129}I/^{127}I)_0$ ratio. In light of the observed anomalies in the isotopic composition of other elements in meteorites (e.g. ^{16}O) [31], which also indicate an inhomogeneous solar nebula, it is not too demanding to expect that such inhomogeneities existed in the iodine isotopy as well.

Acknowledgements

We thank Dr. P. Pellas from the Muséum National d'Histoire Naturelle in Paris for using his expertise in providing us with meteorite samples which met the criteria of minimum shock and weathering, and suggesting and encouraging us to purpose this undertaking. We thank as well his colleague Dr. D. Storzer for his stimulating discussions. We also wish to thank Drs. D. D. Clayton and E. K. Jessberger for their valuable discussions and encouragement.

The irradiations were supported by the Gesellschaft für Kernforschung mbH, Karlsruhe. We gratefully acknowledge Drs. Wolf and Rottmann at the FR 2 reactor in Karlsruhe for their friendly assistance.

We thank Mr. Oberfrank for assistance with the Fe-wire activity measurements. Finally, a special thanks goes to H. Urmitzer and A. Fellinger for typing the manuscript.

[1] P. M. Jeffery and J. H. Reynolds, J. Geophys. Res. **66**, 3582 (1961).
[2] F. A. Podosek, Geochim. Cosmochim. Acta **34**, 341 (1970).
[3] A. G. W. Cameron, Icarus **1**, 13 (1962).
[4] W. R. Van Schmus and J. A. Wood, Geochim. Cosmochim. Acta **31**, 747 (1967).
[5] G. F. Herzog, E. Anders, E. C. Alexander, Jr., P. K. Davies, and R. S. Lewis, Sicence **180**, 489 (1973).
[6] R. S. Lewis and E. A. Anders, Proc. Nat. Acad. Sci. USA **72**, 268 (1975).
[7] R. J. Drozd and F. A. Podosek, Earth Planet. Sci. Lett. **31**, 15 (1976).
[8] D. Heymann, Icarus **6**, 189 (1967).
[9] P. Pellas, personal communication.
[10] J. Jordan, T. Kirsten, and H. Richter, Meteoritics **12**, 269 (1977).

[11] J. Jordan, T. Kirsten, and H. Richter, Meteoritics **13**, 506 (1978).
[12] T. Kirsten, J. Jordan, H. Richter, P. Pellas, and D. Storzer, U.S. Geol. Survey Open-File Rep. **78-701**, 215 (1978).
[13] I. Flohs, J. Jordan, and T. Staudacher, 42nd Meteoritical Soc. Abs. (1979).
[14] H. Haag, Masters Thesis, Max-Planck-Institut für Kernphysik, Heidelberg 1975.
[15] F. A. Podosek, J. C. Huneke, D. S. Burnett, and G.J. Wasserburg, Earth Planet. Sci. Lett. **10**, 199 (1971).
[16] K. Marti, P. Eberhardt, and J. Geiss, Z. Naturforsch. **21a**, 398 (1966).
[17] G. Rudstam, Z. Naturforsch. **21a**, 1027 (1966).
[18] M. W. Rowe, D. D. Bogard, and P. K. Kuroda, J. Geophys. Res. **71**, 4679 (1966).
[19] M. W. Rowe, Earth Planet. Sci. Lett. **2**, 92 (1967).
[20] C. M. Hohenberg, M. N. Munk, and J. H. Reynolds, J. Geophys. Res. **72**, 3139 (1967).
[21] P. Eberhardt, J. Geiss, H. Graf, N. Grögler, M. D. Mendia, M. Mörgeli, H. Schwaller, and A. Stettler, Proc. Third Lunar Sci. Conf., 1821-1856, 1972.
[22] O. A. Nier, Phys. Rev. **79**, 450 (1950).
[23] A. G. W. Cameron, Space Sci. Rev. **15**, 121 (1973).
[24] D. York, Can. J. Phys. **44**, 1079 (1966).
[25] S. Niemeyer, Geochim. Cosmochim. Acta **43**, 843 (1979).
[26] A. Zaikowski, Meteoritics **13**, 677 (1978).
[27] A. Zaikowski, Tenth Lunar Planet. Sci. Conf. Abs., 1392-1394 (1979).
[28] G. J. Wasserburg and J. C. Huneke, Tenth Lunar Planet. Sci. Conf. Abs., p. 1307-1309 (1979.)
[29] J. C. Huneke, Earth Planet. Sci. Lett. **28**, 407 (1976).
[30] D. D. Clayton, Astrophys. J. **199**, 765 (1975).
[31] F. A. Podosek, Ann. Rev. Astron. **16**, 293 (1978).